UiT The Arctic University of Norway

Faculty of Biosciences, Fisheries and Economics, Department of Arctic and Marine Biology

Gelatinous zooplankton diversity, distribution and seasonality in the northern Barents Sea and Arctic Ocean

Angelo Ciambelli

Master's thesis in Biology, BIO-3950, May 2023

Gelatinous zooplankton diversity, distribution and seasonality in the northern Barents Sea and Arctic Ocean

Angelo Ciambelli

Arctic Marine Ecology

Submission date: May 2023

Supervisor: Camilla Svensen[1]

Co-supervisor: Sanna Majaneva[2], Anette Wold[3]

1 The Arctic University of Norway
2 Norwegian University of Science and Technology
3 Norwegian Polar Institute

The Arctic University of Norway

Department of Arctic and Marine Ecology

Acknowledgements

This master thesis was part of the Nansen Legacy project financed by the Research Council of Norway, the Norwegian Ministry of Education and Research and several participating institutions. It was supervised by professor Camilla Svensen from the Arctic University of Norway (UiT) and co-supervised by chief engineer Anette Wold from the Norvegian Polar Institute (NPI) and Dr. Sanna Majaneva from the University of Science and Technology (NTNU). The thesis was completed at the Department of Arctic and Marine Biology from the Arctic University of Norway (UiT).

Foremost, I would like to thank my supervisors Camilla Svensen, Anette Wold and Sanna Majaneva for giving me the unique opportunity to be involved in the Nansen Legacy project and work on gelatinous zooplankton with them. I would also like to thank them for being very helpful and available when I needed any help or feedback. To my main supervisor, Camilla Svensen – thank you for sharing your wisdom and experience related to organization and scientific writing. To Anette Wold - thank you for being so organized and helpful when I had questions related to the datasets and data analysis. To Sanna Majaneva – thank you for sharing your taxonomy skills and knowledge on gelatinous challenges and teaching me DNA barcoding methods.

Besides, my supervisors, I would like to thank the Research Council of Norway, the Norwegian Ministry of Education and Research and the several participating institutions financing the Nansen Legacy project and giving us the opportunity to complete our knwoledge of the Barents Sea and Arctic Ocean ecosytems.

I would also like to give my sinceres thanks, to the Dr. Angelika Renner for her explanation of the Nansen Legacy CTD data and water masses definitions in the Barents Sea and to the senior ingenior Mari-Ann Østensen from TBS for assisting me when Sanna was occupied, it was really nice to know I could get help anytime.

A special thanks to Louis Munk Klarup, Nicolas Gosset and Kos Pepels for the great working environment, interesting Marine Biology discussions and funny lunch breaks.

Finally, I am very greatful for all the encouragments and support my family gave me. To my family - thank you for your trust and your numerous encouragments at the end of the long writing and data analysis days !

Sincerely, Angelo Ciambelli, Tromso, May 2023

Abstract

Gelatinous zooplankton, here referring to the phylum Cnidaria and Ctenophora and the class Appendicularia are important components of marine ecosystems due to their very diverse diets, life cycles and seasonal dynamics. In the Barents Sea, several studies reviewed the gelatinous zooplankton diversity, yet few studies documented the diversity and distribution patterns between the advected Atlantic Waters (AW) and Polar waters (PW) and no study reviewed the gelatinous zooplankton seasonality over a full year. The aim of this master thesis is to (1) investigate diversity and distribution patterns between the different water masses and regions of the northern Barents Sea and (2) investigate the gelatinous zooplankton seasonality over a whole year in the northern Barents Sea. For this purpose, during the Nansen Legacy project four seasonal surveys covered the full seasonal cycle of the Barents Sea marginal ice zone and collected both biological and physical data, including gelatinous zooplankton. Overall, 31 gelatinous zooplankton taxa were identified. *Fritillaria borealis*, *Oikopleura* sp. and *Aeginopsis laurentii* were the most abundant taxa and AW and PW influenced areas had different seasonal dynamics and composition, which were significantly influenced by the primary production, the zooplankton biomass, the inflow of AW and the latitudes.

Keywords: Gelatinous zooplankton, Barents Sea, Seasonality, Distribution, Atlantic Waters, Polar Waters, Nansen Legacy

Table of Contents

List of Tables

List of Figures

1 Introduction

The Barents Sea is ecologically and economically important (Nilssen, 2003; Sakshaug et al., 2009). It's a shallow shelf sea influenced by the inflow of warm (2°C - 5°C) and high salinity (>35 $g.L^{-1}$) Atlantic Waters passing in the Barents Sea Opening in the South and the inflow of cold (<0°C) and low salinity (<34.4 $g.L^{-1}$) Arctic Waters passing between the archipelago of Svalbard and Novaya Zemlya in the North (Figure 1)(Drinkwater, 2011; Loeng & Drinkwater, 2007; Skagseth, 2008). As a result, it is a diversity hotspot and both Arctic and Atlantic expatriate species co-exist, for example, *Calanus finmarchicus* and *Calanus glacialis* (Melle & Skjoldal, 1998). Moreover, due to the seasonal light regime, seasonal ice melt and the inflow of Atlantic Waters replenishing the nutrients, the primary production and bloom activity in most regions of the Barents Sea is peaking and high between May to June, leading to high secondary production and fish stocks (Loeng & Drinkwater, 2007; Rey, 1985; Wassmann et al., 1999). Some of the fishes are commercially important and are exploited by fisheries, for example, cod (*Gadus morhua*), capelin (*Mallotus villosus*) and haddock (*Melanogrammus aeglefinus*) (Eriksen et al., 2018). These fisheries are some of the largest fisheries in the world making the Barents Sea particularly important for the economy of neighbouring countries, Russia and Norway (Eriksen, Gjøsæter, et al., 2018; Nilssen, 2003).

However, in the last decade human perturbances have increased in the Barents Sea (shipping, oil and gas exploration, tourism) and with climate changes, the temperatures of the Barents Sea have increased (Barton et al., 2018; Ellingsen et al., 2008; Holthus et al., 2013; Loeng et al., 2005). In the future, further warming is predicted due to an increase in both the volume and temperature of the Atlantic inflow (Slagstad et al., 2015). The warming of the Barents Sea will likely cause a decrease of the annual sea ice concentration, an increase in primary production and a shift northward in habitats is predicted (Slagstad et al., 2015). As a result, Atlantic and boreal species will be found at higher latitudes and more in the eastern Barents Sea and Arctic species will be more restrained to the Arctic Basins (Fossheim et al., 2015; Slagstad et al., 2015). This can lead to a decline in diversity in the Barents Sea, changes in repartition of the fish stocks and increase in the probability of mismatch between phytoplankton blooms and predator spawning (Asch et al., 2019; Fossheim et al., 2015). Therefore, to assess possible changes and contribute to the conservation and monitoring of the Barents Sea ecosystem, it is crucial to study and understand in detail its community composition and their distribution and seasonal dynamics.

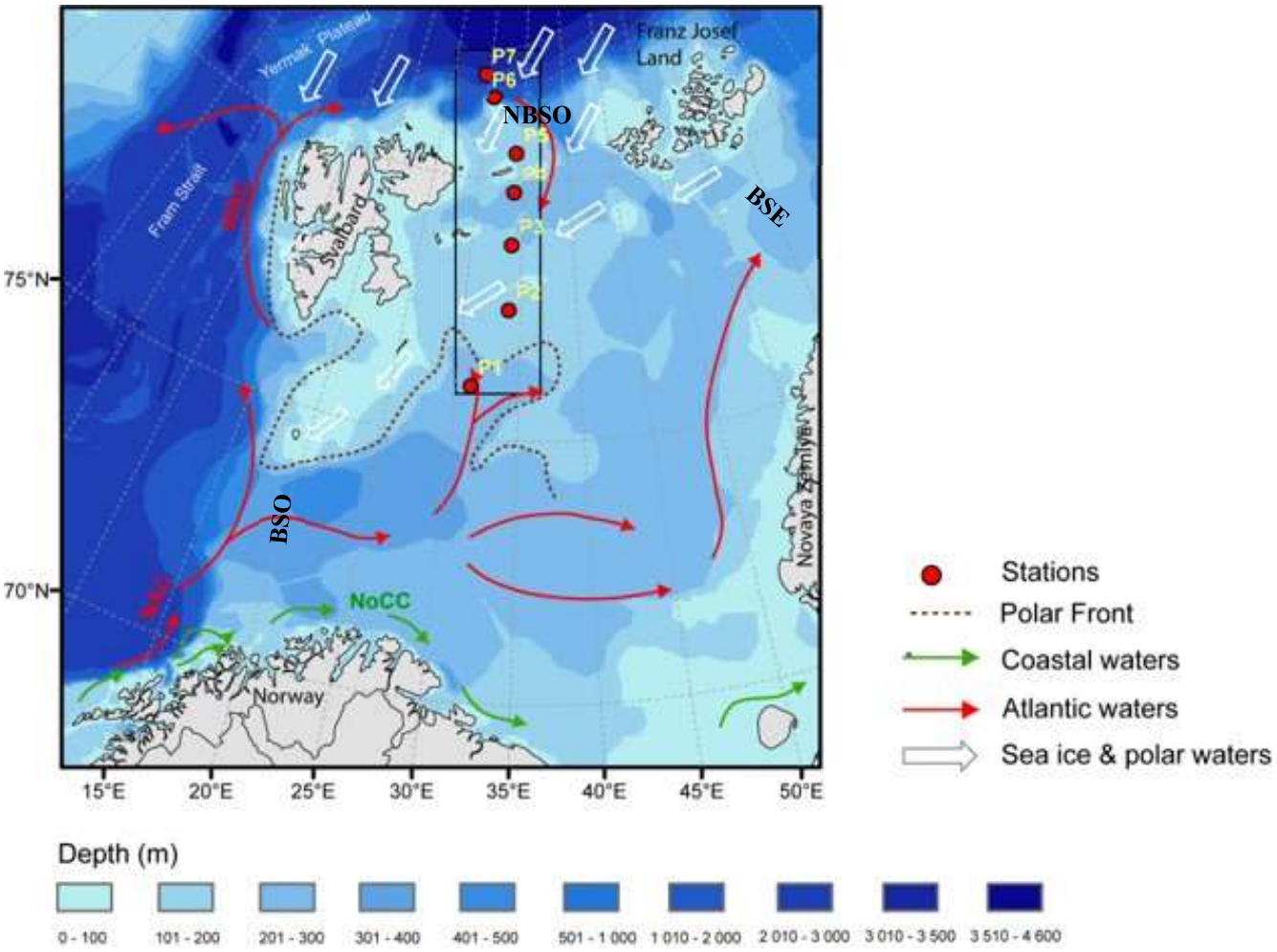

Figure 1 – Sampling stations (red dots) from the seasonal surveys in 2019 and 2021 in the northern Barents Sea. The current systems NAC (Norwegian Atlantic Current), NoCC (North Cape Current), and WSC (West Spitsbergen Current) are indicated in the colours of their respective water masses. The different openings of the Barents Sea BSO (Barents Sea Opening), BSE (Barents Sea Exit), NBSO (Northern Barents Sea Opening) are also included. The figure is modified from Figure 1 in Van Engeland et al. (submitted to Progress in Oceanography).

I will focus, in this study, on the gelatinous zooplankton, a polyphyletic group, composed by translucent and soft body taxa having high-water and low-carbon contents (Pitt & Lucas, 2014). By definition, gelatinous zooplankton commonly includes the phylum Cnidaria, Ctenophora and Chaetognatha as well as the pelagic tunicates (Steinberg & Saba, 2008). However, almost all marine phyla, including Annelida, Mollusca and Arthropoda, contain gelatinous species or life stages (Harbison, 2009). In this study, when referring to gelatinous zooplankton, I will only include the phylum Cnidaria and Ctenophora and the class Appendicularia. It's a very diverse group in terms of sizes, life strategies, life cycles, trophic interactions, distribution and seasonal dynamics (Harbison, 2009; Pitt & Lucas, 2014).

1.1 Life cycles and seasonality

Gelatinous zooplankton life cycles are very diverse, sometimes very complex and differ between the phylogenetic groups (Arai et al., 2017; Collins, 2002; Deibel & Lowen, 2012). Most Cnidaria, namely the classes Cubozoa and Scyphozoa and the orders Leptomedusae and Anthomedusae, during their life cycle alternate between short lifespan medusae and perennial polyp forms (Figure 2)(Collins, 2002; Lucas et al., 2012; Pitt & Lucas, 2014). Polyp life stages are often colonial with specialized members, they reproduce mostly asexually through metagenesis and strobilation and are mostly benthic and sessile (Arai et al., 2017; Boero et al., 2008; Collins, 2002). Medusae life stages on the other hand are free living individuals, they reproduce sexually and are only pelagic (Boero et al., 2008; Collins, 2002). Some other Cnidaria taxa, have either no polyp stage (e.g. Trachymedusae, Narcomedusae) or no medusae stage (e.g. Hydridae, Siphonophorae)(Arai et al., 2017; Collins, 2002). Most Cnidarians are meroplanktonic, as they have a both benthic and pelagic life stages in their life cycle.

Cnidaria life cycle durations vary between taxa and for example, the Schypozoa *Cyanea nozakii* has a one-year life cycle whereas the Hydrozoan *Aglantha digitale* can possibly have multiple generation per year (Ikeda & Imamura, 1996; Mańko et al., 2020; Pertsova et al., 2006; Thein et al., 2013). Additionally, Cnidaria sexual and asexual reproduction have been shown in previous studies to be influenced by temperature, food availability and light regimes (Lucas et al., 2012; Pertsova et al., 2006; Purcell et al., 2009; Thein et al., 2013).

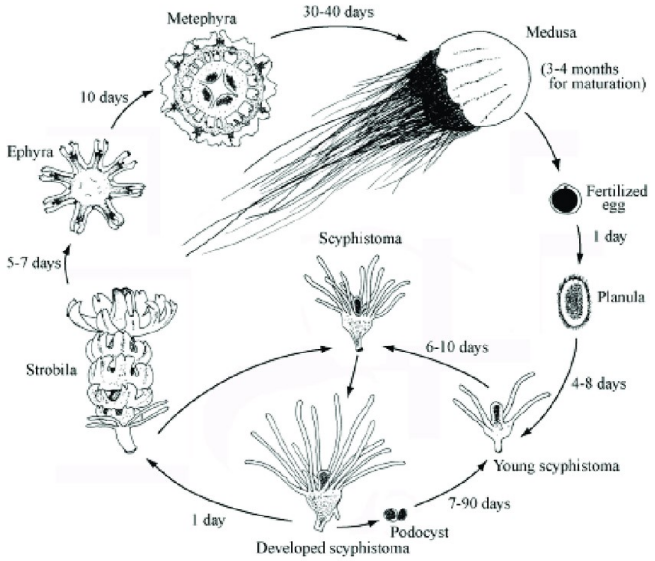

Figure 2 – Nemopilema normurai (Schypozoa) life cycle, alternating between poylp stages (Scyphistoma) and medusae life stage (Medusa). From Kawahara et al. (2006)

Ctenophora are holoplanktonic and will reproduce sexually possibly multiple time per year by adults releasing sperm and eggs in the surrounding water (Arai et al., 2017; Larson, 1986; Zelickman, 1972). If fertilized, the eggs will grow into a cydippid larva and then into an adult (Figure 3). Most Ctenophora are self-fertile hermaphrodites, have a rapid gametogenesis (~2 days) and high fecundity (Greve, 1970; Reeve & Walter, 1979). Some Ctenophora species, such as *Mnemiopsis leidyi,* can also conduct larval reproduction (dissogeny) where larvae can produce functional gametes (Edgar et al., 2022; Martindale & Henry, 2015). Growth and development of Ctenophora has been shown to be highly influenced by food availability (Kremer & Reeve, 1989).

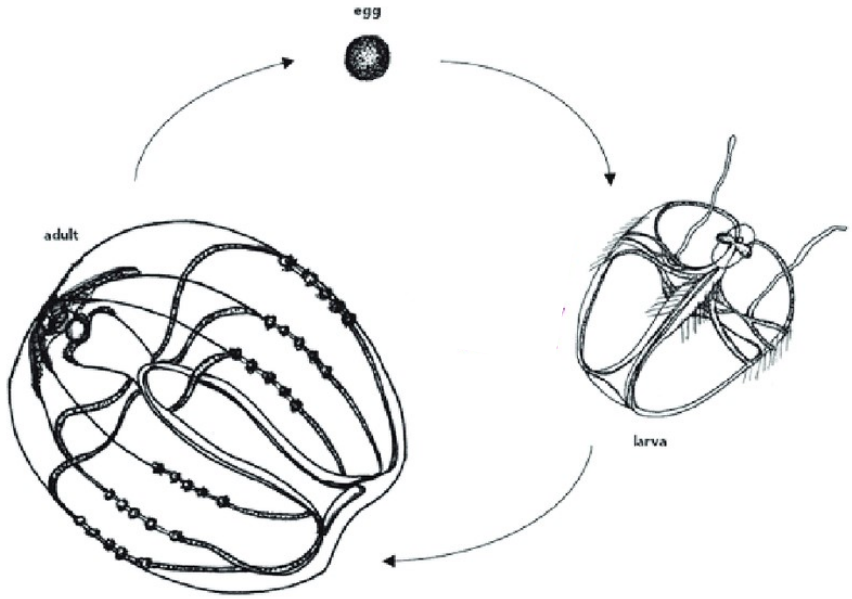

Figure 3 – Mnemiopsis leidyi (Ctenophora) life cycle. Including the egg, cydippid larva (larva) and adult life stages. From Arai et al. (2017)

Appendicularia have a relatively simple life cycle with direct development, they are semelparous, holoplanktonic and protandric hermaphrodites (Deibel & Lowen, 2012). They reproduce sexually, adults produce eggs inside their body then their body wall rupture and the adults die releasing the unfertilized eggs in the surrounding water (Figure 4)(Deibel & Lowen, 2012). Then if the eggs are fertilized, they hatch into a tadpole larva that will grow into an adult (Figure 4)(Deibel & Lowen, 2012). Appendicularia development rates are documented to be fast compared to other tunicates and it takes only some hours to a day for the first filtration house to be inflated (Deibel & Lowen, 2012; Troedsson et al., 2002). Additionally, it has been shown, that their generation time decrease and egg production increase with increasing temperature and food availability (Deibel & Lowen, 2012).

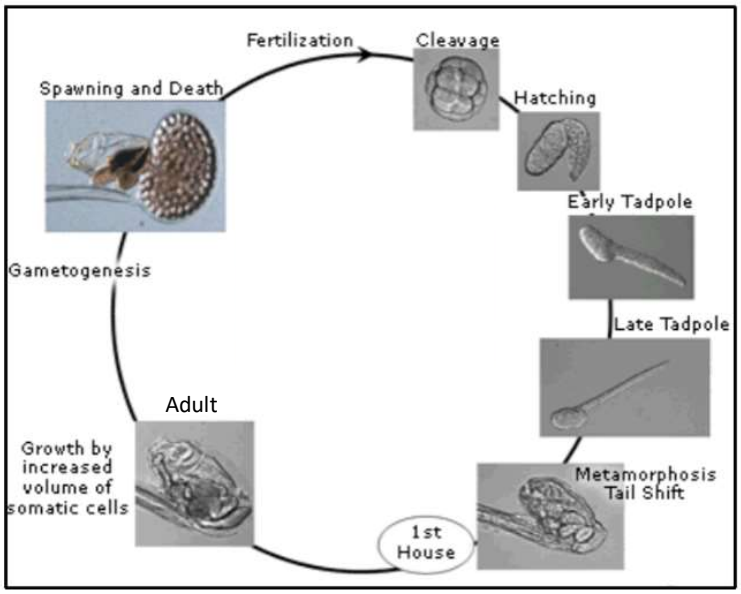

Figure 4 – Oikopleura dioica (Appendicularia) life cycle. Including the tadpole larva (Early Tadpole & Late Tadpole) and adult life stages. It also includes interesting life history events such as the death of the indidual by releasing the eggs (Spawning and Death) and the first inflated filtration house (1st House). From Deibel & Lowen (2012).

Despite very different life cycles, most gelatinous zooplankton taxa increase in abundance and biomass when the environmental conditions, such as food availability, primary production and temperature are suitable (Boero et al., 2008; Lucas et al., 2014; K. Raskoff et al., 2003). For some taxa, the increases in abundance can be very sharp, leading to population outbreaks and swarms of individuals (true bloom or apparent bloom) (Pitt & Lucas, 2014). These swarms of individuals are often due to life cycle characteristics, notably, fast development rates, high fecundity, rapid gametogenesis and asexual reproduction (Deibel & Lowen, 2012; Pitt & Lucas, 2014). In this case they are called true blooms. However, they may also be initiated by the aggregation of individuals due to advections, currents and behaviours (Graham et al., 2001; Pitt & Lucas, 2014). In which case they are called apparent blooms. Making the distinction between apparent blooms, true blooms or blooms appearing due to the combination of true and apparent blooms is difficult, as the number of births, deaths, immigrants and emigrants should be estimated in case of the accumulation of organisms (Pitt & Lucas, 2014). As a result, it's difficult to identify the origin of the gelatinous zooplankton seasonal variations in abundance.

At higher latitudes and in the Barents Sea the growth, development, spawning, reproduction and accumulation of most gelatinous zooplankton taxa is related to the seasonal increase in temperature and light exposure coinciding with the periods of high primary productivity (Kremer & Reeve, 1989; Purcell et al., 2009; Zelickman, 1972). Hence, highest

abundances are often reached in spring and summer (Falkenhaug, 1996; Hosia & Båmstedt, 2007; Larson, 1986; Pertsova et al., 2006).

1.2 Trophic interactions

Gelatinous zooplankton have an important role in the marine food web by exerting top-down control on their prey population and structuring the food web (Jaspers et al., 2015; Pitt & Lucas, 2014). They are both carnivores and herbivores feeding on a wide variety of prey. They are known for example to feed on fish larvae or eggs, zooplankton, phytoplankton and bacteria (Alvariño, 1985; Bouillon et al., 2004; Purcell & Arai, 2001). The consumption rate of their prey is generally less than 10% of the prey population, but it can reach more than 50% during bloom periods, hence, they could occasionally and locally decimate their prey population (Alldredge, 1984; Majaneva et al., 2013; Pagès et al., 1996; Reeve et al., 1978). Such events can cause a temporal regime shift from a crustacean to a jelly-dominated system (Hwang et al., 2013; Yilmaz, 2015).

Historically, gelatinous zooplankton have been considered a trophic dead end (Verity & Smetacek, 1996). However, recently it has been documented that they are also preyed by crustaceans, seabirds and commercially and ecologically important fishes. For example, in the Barents Sea, the species *Gadus morhua* (cod), *Salmo salar* (salmon), *Cyclopterus lumpus (*Lumpfish), *Anarhichas denticulatus* (Wolffish) and *Pandalus borealis* were reported to feed on gelatinous taxa (Eriksen et al., 2020; Eriksen, Gjøsæter, et al., 2018; Hamilton, 2016) (Urban et al., 2022). Hence, gelatinous zooplanktons are in fact a channel of energy between low trophic levels and higher trophic levels (Jaspers et al., 2015).

Gelatinous zooplanktons are considered to have a negative impact on fisheries because they feed on fish larvae and compete with zooplanktivorous fishes and larvae, hence reducing the fish stocks (Brodeur et al., 2008, 2011). This have been shown to have a high impact on already weakened and overexploited fish stocks where ultimately gelatinous zooplankton overtake fish in the ecosystem (Lynam et al., 2006; Oguz & Gilbert, 2007). However, since they can also be prey of commercially important species, it may not be easy to conclude that gelatinous have a negative impact on fisheries as it will depend on the species present. Hence, reinforcing the need of good monitoring of the gelatinous zooplankton community.

1.3 Sampling, conservation and identification challenges

Historically, gelatinous zooplankton have been overlooked in the world oceans and in the Barents Sea due to sampling, identification and conservation challenges (Majaneva & Majaneva, 2013; K. Raskoff et al., 2003; Swanberg & Båmstedt, 1991a).

Gelatinous zooplankton have a wide range of sizes, ranging from less than a millimeter to more than a meter, and covering the whole range will require different sampling gears (Agassiz, 1865; Harbison, 2009). They are fragile and often damaged when sampled with plankton nets and trawls, leading to an underestimation of the fragile taxa (e.g. Appendicularia). Also, due to their high transparency, some species can be hard to observe using ROV (e.g. *Aglantha digitale*) (Raskoff et al., 2005). Hence, using multiple methods (nets, ROV and diving) is recommended to prevent sampling biases due to the differences in size, transparency and fragility between gelatinous taxa (Raskoff et al., 2003).

The identification literature is often incomplete and focused on specific, often adult, life stages. As a result, identifying earlier life stages can be difficult and sometimes impossible. DNA barcoding methods are starting to be more used, but the lack of reference databases and amplification protocols make the application of DNA barcoding methods difficult for some taxa (Jucker & Havermans, 2022; Ortman et al., 2010).

Some gelatinous zooplankton taxa are altered in conservative mediums, they can lose taxonomic features and shrink, making their identification difficult or impossible (Mutlu, 1996). Nowadays, despite the bad conservation of some taxa it's sometimes possible to identify them using DNA barcoding methods (Ortman et al., 2010).

1.4 Aim of my study

In recent years gelatinous zooplankton have drawn more attention due to their negative impacts on fisheries, aquaculture, and tourism (Halsband et al., 2018; Yilmaz, 2015). Recent papers, highlight that given the importance of gelatinous zooplankton, future ecosystem-based management efforts should include standardized, consistent and coordinated monitoring of gelatinous zooplankton (Pierson et al., 2020). In the Barents Sea, several studies have reviewed the gelatinous zooplankton diversity, yet few studies reviewed the diversity and distribution patterns between the different Barents Sea water masses and as far as I known no study

documented the gelatinous zooplankton seasonality over a whole year in the Barents Sea (Blachowiak-Samolyk, 2008; Dvoretsky & Dvoretsky, 2010; Eriksen, Bogstad, et al., 2018; Eriksen et al., 2012; Mańko et al., 2015; Ronowicz et al., 2015; Yaragina et al., 2021; Zelickman, 1972). The Nansen Legacy project covered with four seasonal surveys the full seasonal cycle of the Barents Sea marginal ice zone, a vast area, ranging from the central Barents Sea to the Arctic Ocean Nansen Basin (Figure 1). During the four surveys, both biological and physical data were collected, including gelatinous zooplankton, permitting the investigation of their diversity, distribution and seasonal dynamics. The aim of this master thesis is to (1) investigate diversity and distribution patterns between the different water masses and regions from the northern Barents Sea and (2) investigate the gelatinous zooplankton seasonality over a whole year in the northern Barents Sea.

2 Material and methods

2.1 Sampling area

The sampling was conducted east of Svalbard from the central Barents Sea to the Nansen Basin in a region known for having advections of both Atlantic and Arctic Waters (Figure 1)(Lind & Ingvaldsen, 2012; Loeng, 1991).

Relatively warm (2°C - 5°C) and high salinity (> 35g.L^{-1}) Atlantic Waters are transported into the Barents Sea by two flowing branches (Lind & Ingvaldsen, 2012; Loeng, 1991). The first Atlantic Water branch is slow and wide, it comes from the Norwegian Atlantic Current (NAC) and enters the Barents Sea by the Barents Sea Opening (BSO) (Loeng, 1991). It flows eastward over the Barents Sea shelf and exits into the Arctic Ocean east of Franz Josef Land (Figure 1)(Rudels et al., 2015). The second Atlantic Water branch is relatively fast and narrow and originates from the West Spitzbergen Current (WSC) (Aksenov et al., 2011). It flows eastward along the Barents Sea continental slope under Arctic Waters and sometimes enters the Barents Sea through the Northern Barents Sea Opening (NBSO) (Figure 1)(Lind & Ingvaldsen, 2012).

Relatively cold (< 0°C) and low salinity (< 34.4 g.L^{-1}) Arctic Waters are advected from the Arctic Ocean (Loeng, 1991). They enter the Barents Sea through the North Barents Sea Opening (NBSO) and Barents Sea Exit (BSE) and flow westward over the northern Barents Sea until the Spitzbergen Bank (Figure 1)(Loeng, 1991).

The Atlantic Waters in the south and Arctic Waters in the north are separated by the oceanic Polar Front (Loeng, 1991). This Polar Front is located in my study area between the central Barents Sea station P1 and the northwest Barents Sea station P2 (Figure 1). The southern Barents Sea, south of the Polar Front is highly influenced by the warm Atlantic Waters (Loeng, 1991). Whereas, the northern Barents Sea, north of the Polar front is highly influenced by the cold Arctic Waters and is seasonally ice-covered (Kvingedal, 2005; Loeng, 1991).

2.2 Sampling design

During the Nansen Legacy campaign, four cruises with R/V Kronprins Haakon covered different seasons, Q3 (late Summer) and Q4 (early Winter) were sampled in August 2019 and

December 2019. The quarters Q1 (late Winter) and Q2 (Spring) were sampled in March 2021 and May 2021, two years later due to the Coronavirus pandemic.

During each cruise physical and biological data were collected at 7 stations (P1-P7) along a transect from the central Barents Sea, south of the Polar Front (P1; 76° 0' 0" N, 31° 13' 10.92" E) to the Arctic Ocean (P7; 81° 59' 50.64" N, 29° 58' 48" E) (Figure 1).

Gelatinous zooplankton samples were collected using Methot-Isaac-Kidd ring net (MIK net) (3.15m^2 aperture, 13-m long net with 1500µm pore size and a 500µm mesh in the last meter) fitted with a 10-L cod end and MultiNet Midi (HydroBios, opening: 0.25m^2, net length: 2.50m). The MIK nets were used to collect the macrozooplankton (2 to 20mm) at every station of the transect and quarter of the year (except Q3-P6, Q1-P1, Q2-P2). They were hauled vertically from 20 meters of the seafloor to the surface at a speed of 1.5$m.s^{-1}$ (AeN protocol). The MultiNets with both 64µm and 180µm mesh sizes were used to collect both small mesozooplankton (0.1 to 0.2mm) and larger mesozooplankton (0.2 to 2mm) (Makoto & Tsutomu, 1984). They were hauled vertically at a speed of 0.3 and 0.5$m.s^{-1}$ for every quarter of the year over the intervals bottom-200m, 200-100m, 100-50m, 50-20m, 20-0m for the stations P1 to P5 and the intervals bottom-600m, 600-200m, 200-50m, 50-20m, 20-0m for the stations P6 and P7.

2.3 Sample processing and storage

The gelatinous zooplanktons from the MIK net were manually picked out immediately using filtering spoons or wide-mouthed pipettes on board. The individuals were identified to the highest taxonomic level possible and counted. Then selected individuals (up to 12 individuals per taxa) were pictured, weighted, volume measured and stored in >96% non-denatured EtOH at -20°C for possible DNA analysis. From some cruises, the total volume and total wet biomass per station of the gelatinous species was also measured.

The remaining MIK net sample was divided in two, one half for taxonomy analyses at the Institute of Marine Research (IMR) and one half for metabarcoding at the Arctic university of Norway (UiT). The missed picked out gelatinous from the MIK nets were obtained from IMR, but they were very few and their identification resolution was low, so they were not included in the analysis. The metabarcoding data were not used in this project.

Further identification of the MIK net individuals was done with morphological examinations using a stereomicroscope at the Trondheim Biological Station (TBS) and by examining the on-board pictures. Mills & Haddock (2007) and Licandro & Lindsay (2017) were used for the identification of Ctenophora and "The ID guide for pelagic gelatinous zooplankton (Cnidaria and Ctenophora) from the Norwegian Arctic" made by Aino Hosia, Luis Martell and Sanna Majaneva (Unpublished) was used for the identification of both Cnidaria and Ctenophora. When the identification was still unsure, a tissue sample was taken for possible DNA analysis (See 2.5 Laboratory analysis).

MultiNet samples (including gelatinous organisms) were concentrated on sieves (64 µm and 180 µm respectively), gently flushed with filtered seawater before being preserved in 4 % formaldehyde free from acid. They were analysed at the Institute of Oceanology of the Polish Academy of Sciences (IOPAN). The organisms were identified and counted under a stereomicroscope equipped with an ocular micrometer according to standard procedures (Harris et al. 2000).

2.4 Additional data collection

A shipboard conductivity, temperature and depth profiler (Seabird 911 plus CTD) was used to get the physical properties (conductivity, temperature and depth) of the water column at all stations during all cruises. It was hauled down from the surface to 5-10m above bottom and then up to the surface again. It was mounted on a 24-bottles rosette system and equipped with a double set of temperature and conductivity sensors, pressure sensor, oxygen and fluorescence sensors, an altimeter and a turbidity and PAR sensor (Nansen Legacy protocol). Water samples were collected at selected depths from 0 to 100 meters for Chlorophyll *a* (Chl *a*) measurements using a fluorometer. The Chlorophyll *a* standing stock ($mg.m^{-2}$) was integrated for every station over the first 50 meters of the water column using the trapezoidal rule. Protists were also extracted from the water samples and the carbon weight ($gC.m^{-2}$) of the different protist's phylum were calculated by Philipp Assmy.

2.5 Molecular species identification

2.5.1 Tissue sampling & DNA extraction

The tissue sampling and DNA extraction was done on 161 gelatinous individuals that could not be identified using taxonomic methods. The tissue sampling and DNA extraction were both performed in the pre-PCR part of the laboratory in the Trondheim Biological Station (TBS) (Appendix 1).

The tissue samples (~1mm) were collected around the mouth for *Beroe* spp., at the ctenes or the pigmented zones for the Cydippida and at the base of the umbrella from the medusae. The tissue samples were placed in 1mL DNase-free Eppendorf tubes and dried under the ventilation hood. The tools used for the tissue sampling were carefully rinsed three times using tap water between the individuals.

The DNA was extracted using the Chelex rapid-boiling procedure (Granhag et al., 2012). In the dried tissue Eppendorf tubes was added 50 µL of 6% Chelex solution. The tubes were then vortexed (7sec), heated at 98°C for 10minutes and centrifuged at 15 000 $n.min^{-1}$ for 10 minutes. The surnactant (DNA) was finally pipetted into a new DNase-free 1mL Eppendorf tube and stored at -20°C.

2.5.2 DNA amplification

Polymerase Chain Reactions (PCRs) were used to amplify the DNA samples. The PCRs were performed on 118 DNA samples in September 2022 and February 2023 in TBS post-PCR lab using the Applied Biosystems SimpliAmp Thermal Cycler (Appendix 2). Only *Beroe* spp. samples were amplified due to time constraints.

For these *Beroe* spp. samples, the gene coding for the 18S ribosomal RNA (18S rRNA gene) was chosen to be amplified using the pair of primers Kober 18SF (5′CTG GTT GAT CCT GCC AGT AGT3′) and Kober 18SR (5′ GCA GGT TCA CCT ACA GAA ACC3′), respectively the forward and reverse primers (Kober & Nichols, 2007). The PCR wells contained 20µL of solution, consisting in 1µL of DNA material from my extraction, 1µL of Kober 18SF and Kober 18SR and the commercial PCR mix composed by 0.4µL of the *Phire® Hot Start II* polymerase, 4 µL of Phire® reaction buffer (5x buffer), 0.4 µL of dNTP 10 mM, 0.6 µL of 3% DMSO, 11.6 µL of Nuclease free water (dH_2O). Negative controls had 1µL of dH_2O instead of the DNA (Appendix 3).

The PCR DNA amplification started with a first denaturation at 98°C for 5 minutes, followed by 40 cycles including a denaturation at 98°C for 8seconds, annealing at 56°C for 10seconds and synthesis at 72°C for 1minutes. Lastly, there was a final synthesis at 72°C for 5minutes and the PCR ended keeping the PCR products at 4°C until they were taken out (Appendix 3).

The success of the amplifications was then checked by conducting gel-electrophoresis on the PCR products (Appendix 3 & 4).

2.5.3 DNA purification and sequencing

The PCR products successfully amplified were purified using the Cytiva GFX^{tm} PCR DNA and gel purification kit and following the manufacturer standard protocol (Appendix 3). The purified DNA solutions were then sent for forward and reverse Sanger sequencing at Macrogen Europe in Amsterdam (Netherland)(Sanger et al., 1977). In total, 88 purified DNA solutions were sent for sequencing.

2.6 Data Processing & statistical analyses

2.6.1 CTD data processing

Mean temperature and mean salinity at every station and quarter of the year were calculated by averaging the CTD temperature and salinity measurements taken over the whole water column.

The CTD data were also assigned to a water mass using the water masses definitions outlined for the Nansen Legacy project (Sundfjord et al., 2020). In this report they documented the seven different water masses that can be found in the Northern Barents Sea and Nansen Basin. Namely, Polar Water (PW), Warm Polar Water (wPW), Atlantic Water (AW), Modified Atlantic Water (mAW), Cold Barents Sea Deep Water (CBSDW), Intermediate Water (IW) and Eurasian Basin Deep Water (ESDW) (Table 1).

In my analysis, the water masses AW and mAW were combined and called AW and the distinction of ESDW from IW wasn't done. This was performed to reduce the complexity and make the analysis easier.

Table 1 - Water masses definitions and descriptions from Sundfjord et al (2020).

Water mass name	Definition	Description
PW (Polar water)	CT ≤ 0.0°C, σ_0 ≤ 27.97 kg.m^{-3}	Polar Water is formed by the introduction of (cold) sea ice melt water.
wPW (Warm Polar Water)	CT > 0.0°C, S_A < 35.06 g.kg^{-1}	Warm Polar Water can be PW that has been heated through solar radiation or mixing products between AW/mAW and PW.
AW (Atlantic Water)	CT > 2.0°C, S_A ≥ 35.06 g.kg^{-1}	Atlantic Water is relatively warm and saline although not as warm and saline as in the upstream areas
mAW (Modified Atlantic Water)	0.0°C < CT ≤ 2.0°C, S_A ≥ 35.06 g.kg^{-1}	Modified Atlantic Water is AW that lost heat but hasn't been strongly mixed with the surrounding waters.
IW (Intermediate Water)	-1.1°C < CT ≤ 0.0°C, σ_0 > 27.97 kg.m^{-3}	Intermediate Water is colder and typically found at greater depth than AW and mAW. It can also have lower salinities than AW and mAW.
EBDW (Eurasian Basin Deep Water)	-1.1°C < CT ≤ 0.0°C, S_A > 35.06 g.kg^{-1}	Eurasian Basin Deep Water overlaps with IW and is said to be used for stations over 500m isobath.
CBSDW (Cold Barents Sea Deep Water)	CT ≤ -1.1°C, σ_0 > 27.97 kg.m^{-3}	Cold Barents Sea Deep Water is said to be used only for Barents Sea.

The *in-situ* temperature, salinity and pressure measurements were converted into the conservative temperature, absolute salinity and potential density anomaly using the R package **gsw** (Gibbs Sea Water functions).

2.6.2 Biotic data processing

MultiNet and MIK net gelatinous zooplankton abundances (ind.m^{-3}) were obtained by dividing the organism counts by the filtered volume for every sampling event. The filtered volumes (V, m^3) were calculated as follows,

MIK net: V= 3.14m^2 × hauled distance,

MultiNet: V= -1.2681 + 0.3298 × hauled distance.

Where, for the MultiNets, the filtered volume formula is based on a regression between the flow meter readings and the theoretical filtered volumes ($0.25m^2$ × hauled distance). Moreover, MultiNet taxa abundances per station (A) for all taxa were calculated using the formula,

$$A = \sum_{i=1}^{N} (A_i \times W_i),$$

where, N is the number of sampling intervals, A_i is the abundance of the taxon at the i^{th} sampling interval, and W_i is the width of the i^{th} sampling interval.

Missing total counts data in MIK net data were assessed using the pictures from the cruises and the total wet biomass records when they were recorded. Otherwise, it was assumed to be the number of samples taken for DNA analysis when there were less than six DNA samples, as it was the minimum number of DNA samples taken. In the case of more than six DNA samples, the total count was left empty.

The detection/no detection matrix (Appendix 10) was obtained by checking the detection of every taxon in both the MultiNet and MIK net data.

2.6.3 Statistical analysis

Statistical analyses were conducted on the statistical software R.

To compare the abundance distributions obtained from the MultiNet and MIK net a Wilcoxon-Mann-Whitney test was conducted using the R function wilcox.test() (Neuhäuser, 2011). It was statistically significant with a p-value of 1.8×10^{-12}. Hence, the null hypothesis "there are no difference between the MultiNet and MIK net abundances groups" was rejected.

To study the impact of the environmental variables on the gelatinous zooplankton composition, two redundancy analyses (RDA) were conducted using the abundances from the MIK nets and MultiNets. A redundancy analysis is an extension of a multiple regression, they model the effects of an explanatory matrix $X \in \mathcal{M}_{n,m}(\mathbb{R})$ (environmental matrix) on a response matrix $Y \in \mathcal{M}_{n,k}(\mathbb{R})$ (abundance matrix) (Legendre & Legendre, 2012).Where, n is the number of sites, m the number of environmental variables and k the number of taxa. They were conducted using the R-package 'vegan' (Oksanen et al., 2019). The highest available taxonomic resolution was used in the abundance matrixes, but rare taxa were excluded for both

MultiNets and MIK nets (Single individuals, Sarsia species were grouped under *Sarsia* sp.). To do the redundancy analyses, the two abundances matrixes (Appendix 5 & 6) were transformed using Hellinger transformation (Legendre & Gallagher, 2001; Rao, 1995). The environmental table (Appendix 7) was standardized and centered using the R function decostand().

The set of environmental variables used for the redundancy analyses was determined by the biological interest of the variables and the multicollinearity between the variables. The final set of environmental variables included the percentage of AW (AW_perc), the percentage of PW (PW_perc), the percentage of wPW (wPW_perc), the chlorophyll *a* standing stock in the first 50 meter of the water column in $mg.m^{-2}$ (Chla_stock), the total mesozooplankton and macrozooplankton biomass in $mg.m^{-3}$ excluding the gelatinous zooplankton (tot_zooplankton_biomass), the sum of the ciliates and dinoflagellates biomass in $gC.m^{-2}$ (ciliate_dino_biomass), the day of the year (Day_of_year) and the latitude (latitude).

The redundancy analysis models based on MIK net and MultiNet abundances were both statistically significant (p=0.021 and p=0.003) and explained after adjustments regarding the number of variables 22% and 25% of the variations (adjusted r2). In both redundancy analyses, only, the first axis was significant, and the proportion of unexplained variation was high (50% and 52%). Finally, no significant collinearity was detected during the VIF test. The global, axis and terms significance of the redundancy analyses were accessed with permutation tests, using the function anova.cca() from vegan (Borcard et al., 2011). The multicollinearity was checked using the R function vif.cca() from vegan.

2.6.4 DNA sequences analysis

Forward and reverse sequence chromatograms were visually checked and cleaned using Chromas 2.6.6 software. During the cleaning, low quality ends with low quality scores and undefined peak in signal intensity were cut off and uncertain base pairs with low quality scores were changed using the base pair ambiguity code (Cornish-Bowden, 1985). Additionally, sequences with low qualities were discarded.

Cleaned forward and reverse sequences were then assembled using BioEdit 7.2.5 software. During that process twenty-six sequences could not be assembled because they were too short.

A reference library was made using all available Ctenophora 18S rRNA gene sequences (in total 168 sequences, 02/05/2023) from the National Center for Biotechnology Information, GenBank. Additionally, for the root of the tree, two 18S rRNA gene sequences of *Cyanea capillata* and *Aurelia aurita* were extracted from Genbank.

The sequences from my study, the Ctenophora reference library and the root sequences were aligned using MAFFT (Multiple Alignment using Fast Fourier Transform), with a gap penalty of 1.53 and a gap extension penalty of 0.123 (Katoh et al., 2002; Katoh & Standley, 2013; Madeira et al., 2022). The alignment was then checked and cleaned using BioEdit 7.2.5 software. During the cleaning, poorly aligned regions (gaps) and partial sequences were removed, and the sequences ends were trimmed to match the length of my sequences. If interested the final alignment can be checked in the annex.

From the cleaned MAFFT alignment, containing total 141 Ctenophora sequences and four root sequences, a maximum likelihood (GTR+G+I model) phylogenetic tree was made using GARLI 2.0.1019 software and the bootstrap support values or confidence levels of the clades were calculated from 500 replicates (Zwickl, 2006).

3 Results

3.1 Hydrography

Over the four seasons there were similar patterns in the hydrography along the transect. Firstly, the northwest Barents Sea shelf stations P2 to P5 located north from the Polar Front were more influenced by PW and wPW than the rest of the stations (Figure 5A). Hence, they had lower mean temperatures (under 0°C) and mean salinities (under 34.6 $g.L^{-1}$)(Figure 5B & C, Table 1). Moreover, in March and May 2021, there was an increase of wPW in those northwest Barents Sea shelf stations leading to higher temperatures (except in P5, hence leading to colder temperatures).

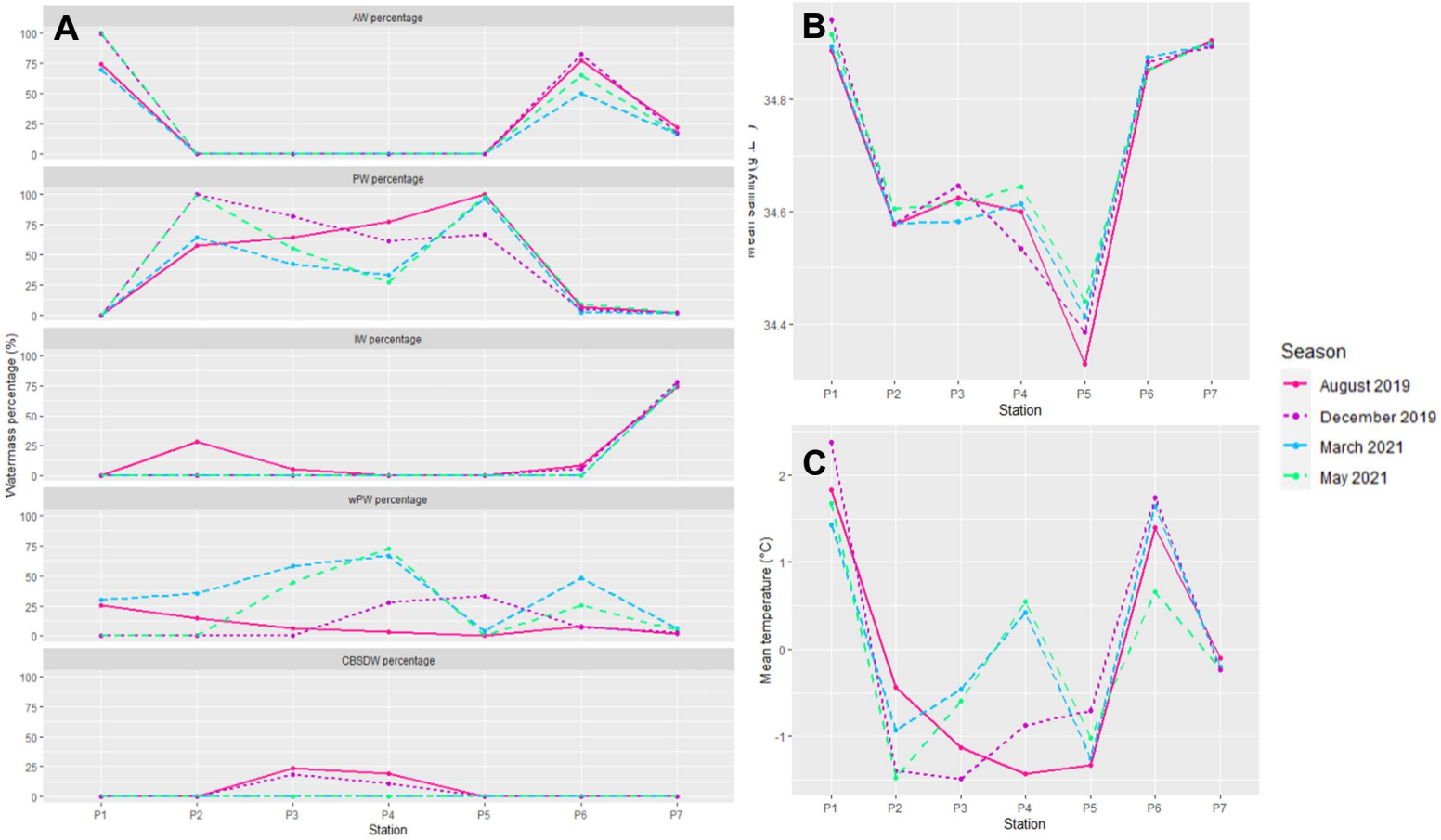

*Figure 5 – Hydrology of the transect (P1-P7) in August 2019 (pink), December 2019 (magenta), March 2021 (cyan) and May 2021 (spring green). Figure **A**, dispay the percentage of every watermasses in percent, EBDW was excluded and mAW was merged into AW. Figure **B**, shows the mean salinity in $g.L^{-1}$. Figure **C**, shows the mean temperature in °Celsius.*

Secondly, the central Barents Sea station (P1), the continental slope station (P6) and the Nansen basin station (P7) had an inflow of Atlantic Water (AW), leading to higher mean temperatures (0°C to 2.5°C) and mean salinities (around 34.9 $g.L^{-1}$) (Figure 1 and 2). The AW was the dominant water mass of the central Barents Sea and Barents Sea continental slope stations and occupied more than 50% of their water column. In the Nansen Basin, the AW was not dominant. Also, notably, in the Barents Sea continental slope station and Nansen Basin station during all seasons, the first hundred meters above the AW were wPW and PW. (Figure 3).

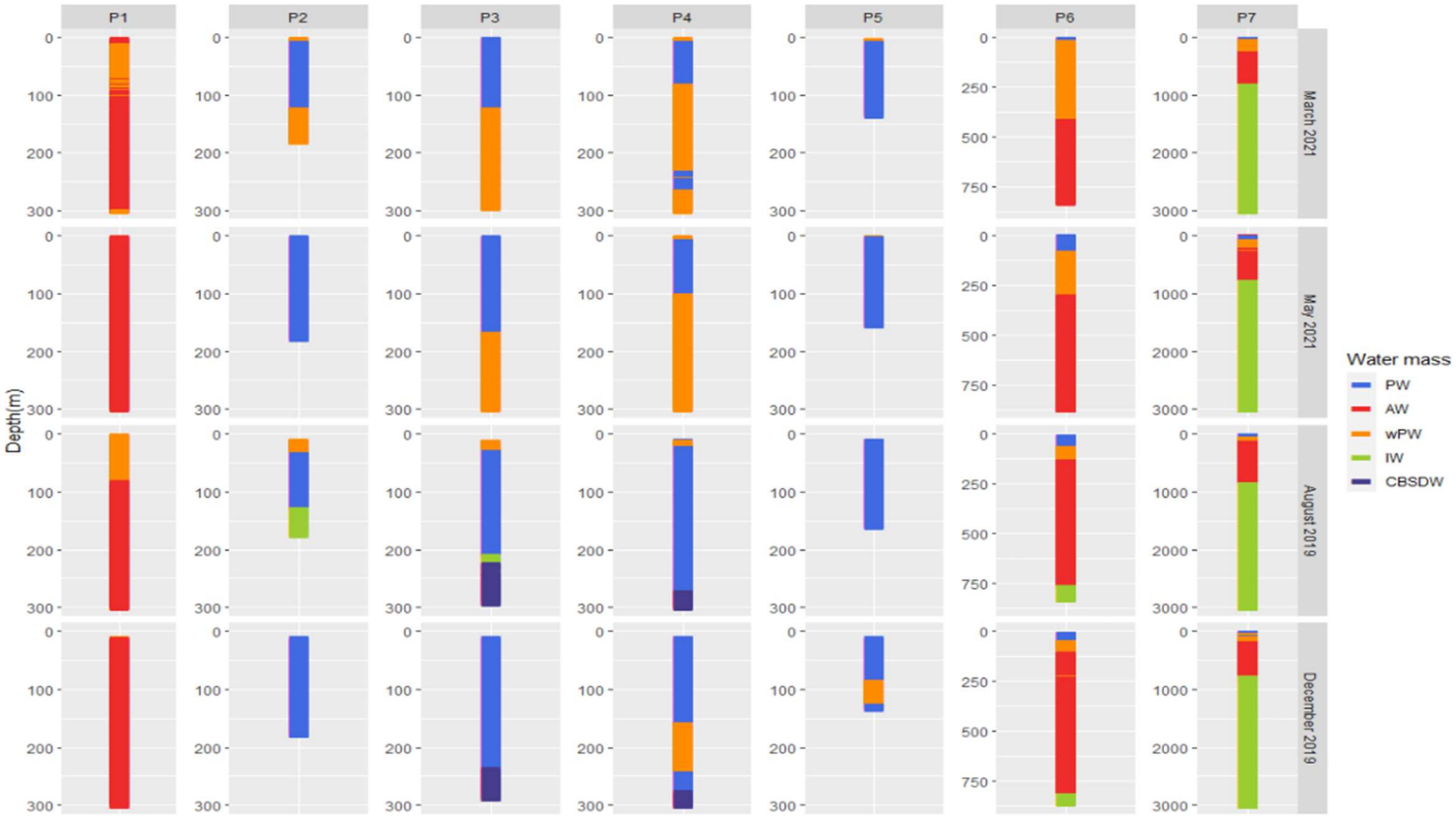

Figure 6 – Watermasses vertical distribution along the transect (P1-P7) in August 2019, December 2019, Mars 2021 and May 2021. The colors represent the different water masses, notably, AW (red), PW (light blue), wPW (orange), IW (green) and CBSDW (dark blue). EBDW were excluded and mAW was merged into AW. For the shelf stations (P1, P2, P3, P4, P5) the maximum depth displayed is 300m and for the off-shelf stations (P6, P7) the whole water column is displayed.

3.2 Chlorophyll a and zooplankton biomass seasonal and spatial patterns

The chlorophyll a stock and microzooplankton biomass peaked in May and August reaching highest abundances in the central Barents Sea and continental slope stations (P1, P6) (Figure 7A & B). The mesozooplankton and macrozooplankton total biomass peaked later in August and December and reached highest biomasses in the northwest Barents Sea shelf stations (P2-P5) (Figure 7C).

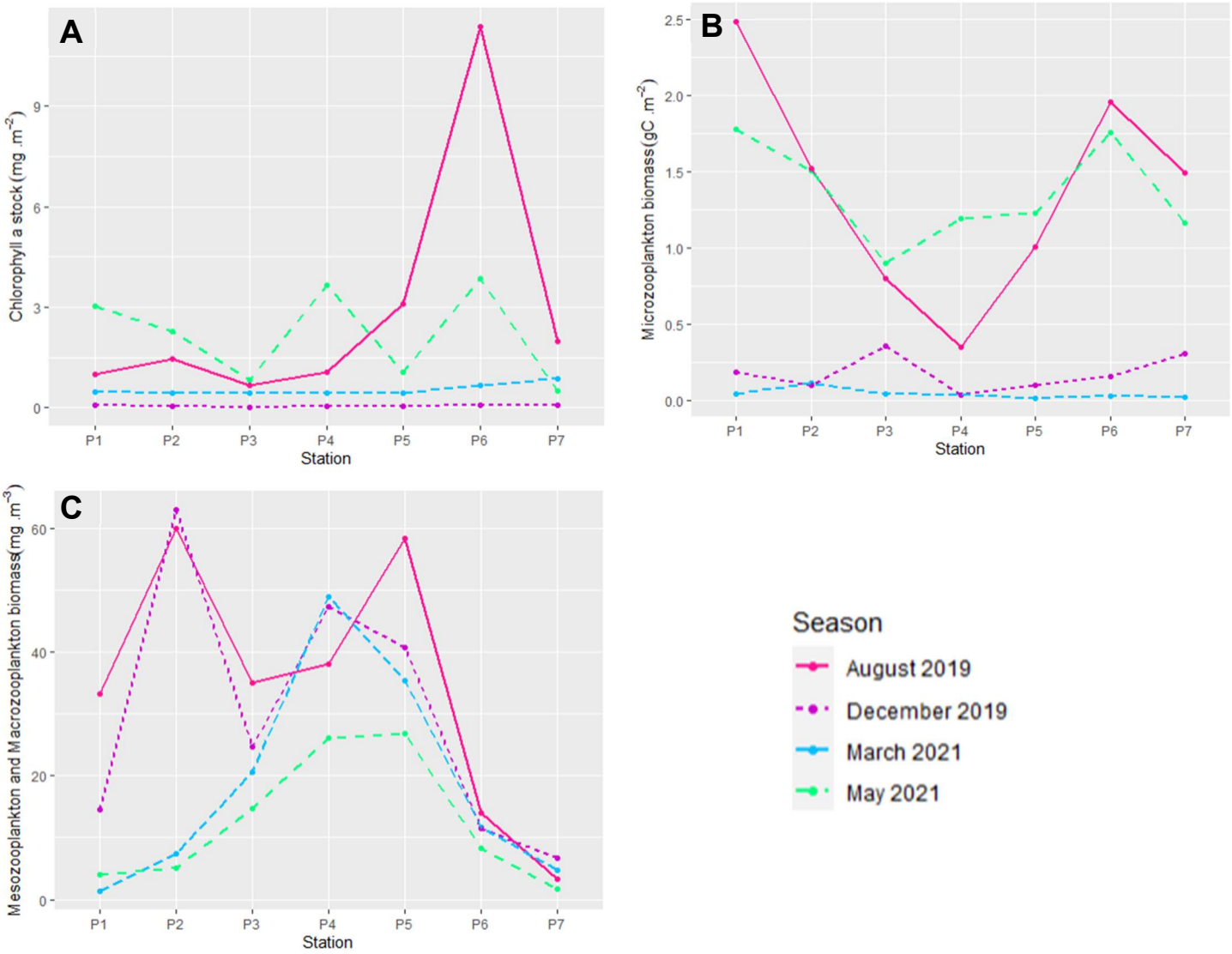

*Figure 7 – Chlorophyll a stock and zooplankton biomass along the transect (P1-P7) in August 2019 (pink), December 2019 (magenta), March 2021 (cyan) and May 2021 (spring green). Figure **A** display the chlorophyll a stock in mg.m^{-2}, It was integrated for the first 50m of the water column. Figure **B**, shows the microzooplankton biomass in gC.m^{-2}, it included the dinoflagellates and cilliates. Figure **C**, shows the mesozooplankton and macrozooplankton biomass in mg.m^{-3}, the gelatinous zooplankton were excluded.*

3.3 Gelatinous zooplankton diversity

For all stations and all seasons, a total of 31 gelatinous taxa were found, of which 23 were identified to species level, four to genus level, two to order level, one to class level and one to phylum level.

The most common and abundant taxa along the transect were the Appendicularia *Fritillaria borealis* and *Oikopleura* sp., the Anthoathecata *Plotocnide borealis*, *Rathkea octopunctata* and *Sarsia* spp., the Narcomedusae *Aeginopsis laurentii*, the Trachymedusae *Aglantha digitale* and *Homoeonema platygonon*, the Beroida *Beroe* spp., the Cydippida *Mertensia ovum* and the Siphonophorae *Dimophyes arctica* (Appendix 8, Figure 8 & 9).

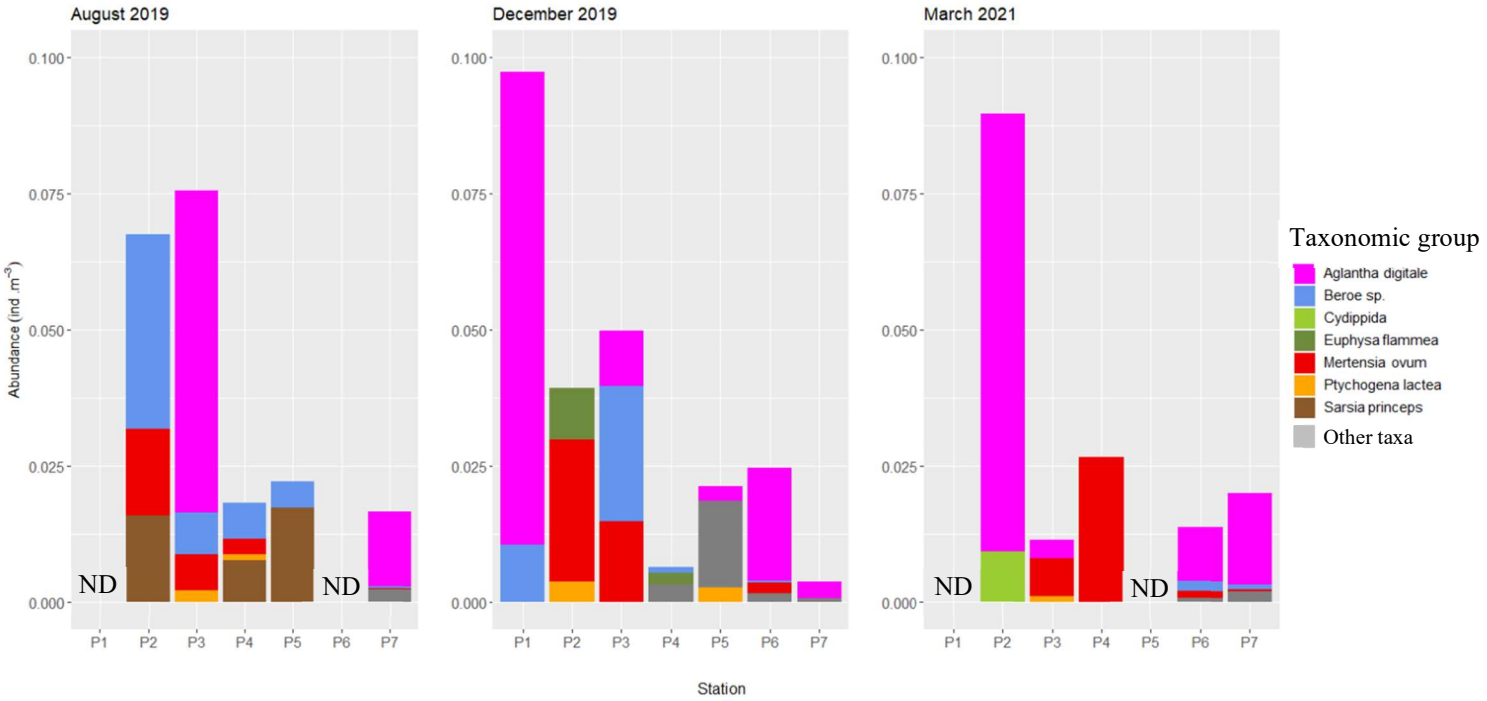

Figure 8 - Gelatinous zooplankton abundance in ind.m^{-3} sampled with a MIK net along the transect (P1-P7) in August 2019, December 2019 and March 2021. Colored by taxonomic groups. Other taxa (grey), included the following taxa Atolla tenella, Botrynema brucei, Botrynema ellinorae, Catablema vescicarium, Cyanea sp., Dryotora glandiformis, Bougainvillia superciliaris, Sarsia sp., Sarsia tubulosa and an unamed cydippid. ND stand for «No Data».

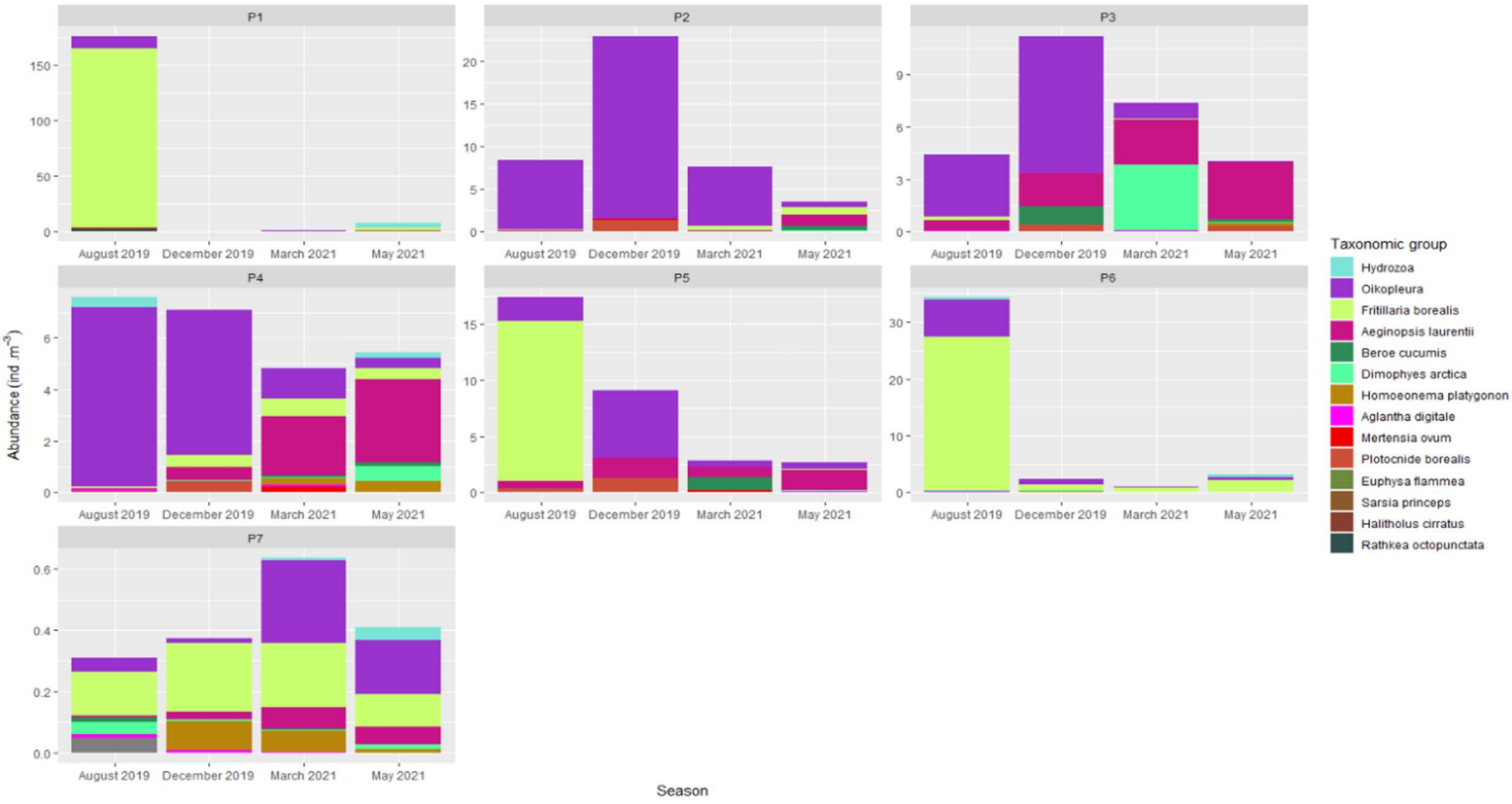

Figure 9 - Gelatinous zooplankton abundance in ind.m^{-3} sampled with a MultiNet in August 2019, December 2019, March 2021 and May 2021 along the transect (P1-P7). Colored by taxonomic groups. Abundance axes range vary within each station and Hydrozoa correspond to Hydrozoa larvae.

The number of taxa was used to estimate the species richness. Such estimator may be biased, and the species richness may be overestimated if the higher taxonomic groups were in fact an already recorded species. Vice versa, the species richness might be underestimated if the higher taxonomic groups included multiple species.

Table 2 – Number of taxa detected along the transect (P1- P7) in August 2019, December 2019, March 2021 and May 2021.

Season	Number of taxa detected
August 2019	25
December 2019	22
March 2021	21
May 2021	19

The species richness of the study area was at its highest in August 2019, with 25 taxa found along the transect (Table 2). The taxonomic richness was highly variable in the central Barents Sea and continental slope stations (P1, P6) and seemed to vary less in the northwest

Barents Sea and Nansen Basin stations (P2, P3, P4, P5, P7) (Figure 10). Also, overall, the shelf station P3, P4 and Nansen Basin station P7 had higher species richness all year around (Figure 10).

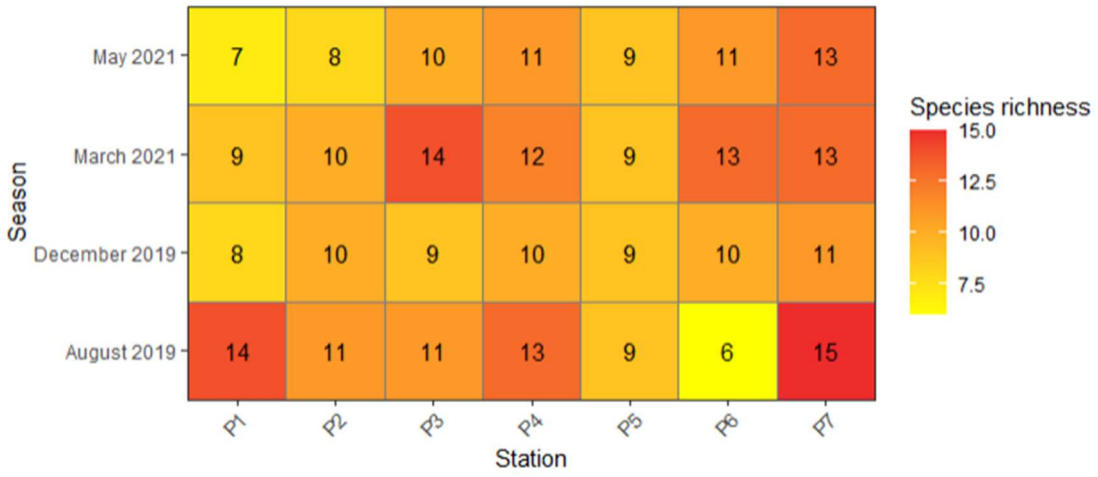

Figure 10 – Gelatinous zooplankton species richness along the transect (P1-P7) in August 2019, December 2019, March 2021 and May 2021. The color range from the lowest lowest species richness (yellow) to the highest species richness (red). Based from both Multinet and MIK net data.

3.4 Gelatinous zooplankton distribution and seasonality

The gelatinous zooplankton MultiNet abundances per station, ranged from 0.3 ind.m^{-3} to 175 ind.m^{-3} (Figure 9, Appendix 6). Whereas the gelatinous zooplankton MIK net abundances per station, ranged from 0.004 to 0.97 ind.m^{-3} (Figure 8). The distribution of the abundances obtained from the MultiNet and MIK net were significantly different (Wilcoxon-Mann-Whitney, p-value 1.8×10^{-12}). Therefore, the gear used to sample the gelatinous zooplankton community had a significant effect on the estimation of the gelatinous zooplankton abundances.

Table 3 - Mean gelatinous zooplankton abundance (ind.m^{-3}) and standard deviation from both MIK net and Multinet data for all seasons (August 2019, December 2019, March 2021, May 2021).

Season	MIK net mean abundance (ind.m^{-3})	MultiNet mean abundance (ind.m^{-3})
August 2019	0.04±0.03	35.5±62.8
December 2019	0.03±0.03	7.6±7.9
March 2021	0.03±0.03	3.6±3
May 2021	No data	3.8±2.4

The total gelatinous zooplankton abundance from the MultiNet was in average, 35.5±62.8 ind.m^{-3} in August 2019, 7.6±7.9 ind.m^{-3} in December 2019, 3.6±3 ind.m^{-3} in March 2021 and 3.8±2.4 ind.m^{-3} in May 2021 (Table 3). The standard deviation and differences in mean highlights a high variation of the gelatinous zooplankton abundances between the stations and seasons, which is confirmed when looking at Figure 9. Additionally, patterns in the gelatinous zooplankton community and dynamics between the AW influenced and PW influenced regions can be observed (Figure 8 & 9).

3.4.1 Central Barents Sea and continental slope

The Central Barents Sea and Barents Sea continental slope had similar gelatinous zooplankton community compositions and seasonal dynamics. The most abundant taxa were, *Fritillaria borealis*, *Oikopleura* sp., Hydrozoa larvae and *Aglantha digitale*. The gelatinous zooplankton total and main taxa abundances peaked seasonally in August and vertically above 100-200m depth, in the surface waters or around the transition between wPW and AW (located between 100 and 200m) (Figure 6 & 9, Appendix 9). The summer gelatinous community was dominated by the appendicularians, *Fritillaria borealis*, *Oikopleura* sp. reaching very high abundances (700 ind.m^{-3} and 120 ind.m^{-3}) in the surface waters and above 100m depth (Appendix 9A).

Despite having similar gelatinous zooplankton community composition and dynamics, the gelatinous zooplankton total abundance peaked higher in the central Barents Sea than on the Barents Sea continental slope, reaching in August 175 ind.m^{-3} compared to 34 ind.m^{-3}, respectively (Figure 9).

In the Central Barents Sea, the meroplanktonic taxa, *Plotocnide borealis* and *Rathkea octopunctata* peaked in abundances in May and August respectively (Figure 11). On the Barents Sea continental slope, *Homoeonema platygonon* and some taxa recorded in low numbers were found, notably, *Sminthea eurygaster*, *Atolla tenella*, *Botrynema ellinorae* and an undescribed cydippid (Figure 11, Appendix 10). *Homoeonema platygonon* peaked seasonally in December (Figure 11).

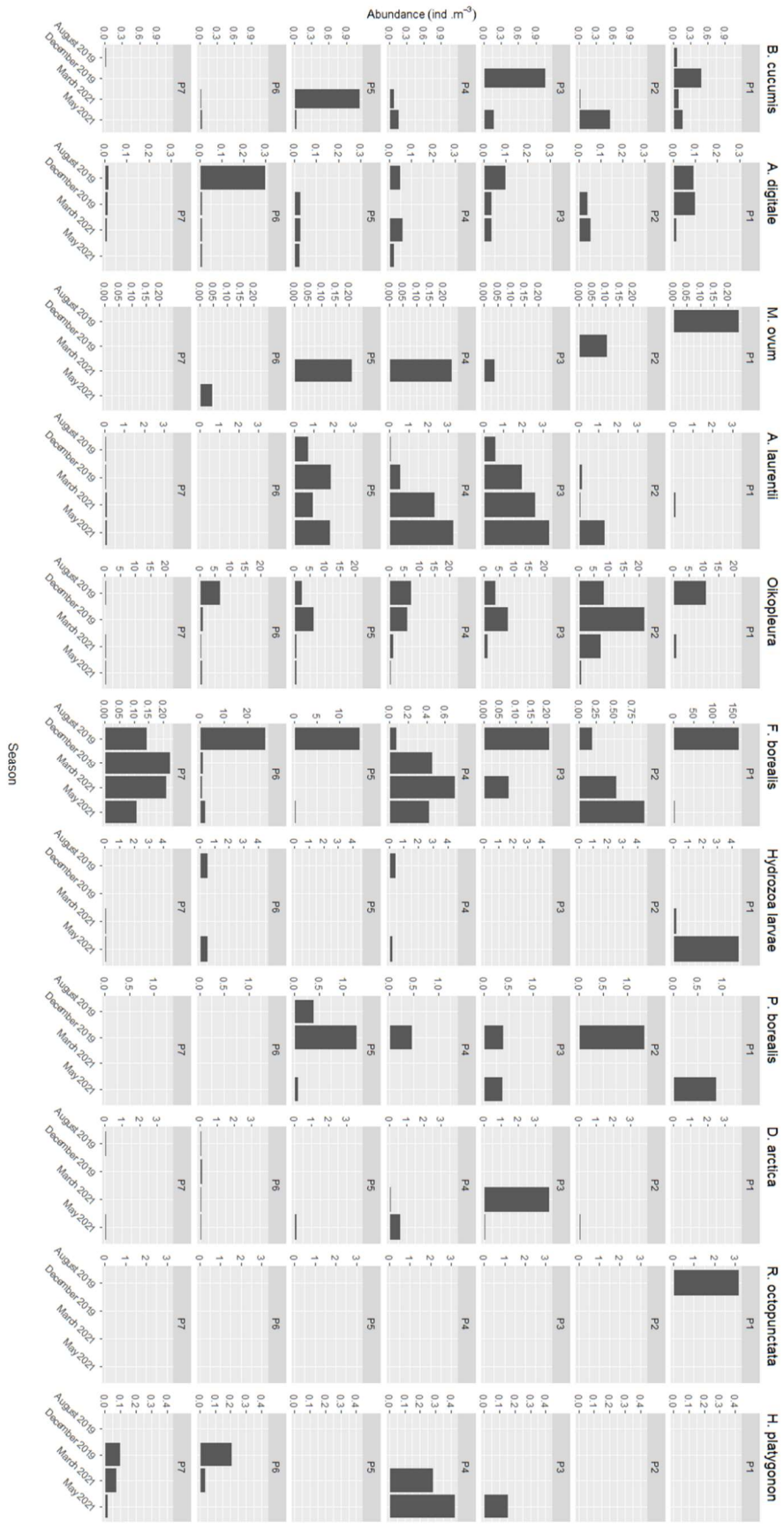

Figure 11 – Common gelatinous zooplankton taxa abundance (ind.m^{-3}) in August 2019, December 2019, March 2021, May 2021 along the transect (P1-P7). Based on MultiNet data.

3.4.2 Northwest Barents Sea shelf

The northwest Barents Sea shelf stations had similar gelatinous zooplankton community compositions and dynamics. They were mostly composed of the taxa, *Oikopleura* sp., *Aeginopsis laurentii*, *Beroe* spp., *Mertensia ovum*, *Fritillaria borealis*, *Dimophyes arctica*, *Sarsia* sp. and *Plotocnide borealis* (Figure 8 & 9). The gelatinous zooplankton total abundance peaked seasonally in August or December and vertically between 50m and 200m, sometimes associated with the transition between PW and wPW (Figure 6 & 9, Appendix 9). In August and December, the gelatinous zooplankton community was mostly dominated by *Oikopleura* sp. which peaked in abundance in December (Figure 9). On the other hand, in March and May, the gelatinous zooplankton community was dominated by *Aeginopsis laurentii* which peaked in abundance in May (Figure 9 & Figure 11).

The abundances of Sarsia sp., *Dimophyes arctica*, *Homoeonema platygonon* and *Plotocnide borealis* varied seasonally (Figure 11). *Dimophyes arctica* peaked in March, *Homoeonema platygonon* peaked in May, Sarsia sp. peaked in August and *Plotocnide borealis* peaked in December (Figure 11).

Additionally, the taxa, *Ptychogena lactea*, *Dryodora Glandiformis*, *Catablema vescicarium*, *Halitholus cirratus*, *Cyanea* sp. and *Bougainvillia superciliaris* were recorded in low numbers (Appendix 10).

3.4.3 Nansen Basin

The Nansen Basin gelatinous zooplankton community most abundant taxa were, *Fritillaria borealis*, *Oikopleura* sp., *Dimophyes arctica*, *Aeginopsis laurentii*, hydrozoa larvae, *Aglantha digitale* and *Homeonema platygonon* (Figure 9). The gelatinous zooplankton total abundances were very low (<1 ind.m^{-3}) and peaked seasonally in March (Figure 9). Vertically the gelatinous zooplankton total abundances peaked in the upper waters (0-200m) or in the upper half of the AW close to the transition with the wPW (200-600m) (Figure 6, Appendix 9).

Moreover, the taxa, *Atolla tenella*, *Botrynema ellinorae*, *Botrynema brucei*, Undescribed cydippid and *Sminthea eurygaster* were recorded in low numbers (Figure 10).

3.5 Environmental factors impact on the gelatinous community composition

Two redundancy analysis (RDA) were made, one with the MIK net abundance data and one with the MultiNet abundance data (Appendix 6 & 7). They both showed that the gelatinous zooplankton community was significantly influenced by environmental factors (respectively, p=0.021 and p=0.003). The gelatinous zooplankton community sampled with the MIK nets was significantly impacted the Chlorophyll a stock and the total mesozooplankton and macrozooplankton biomass (Table 4). Similarly, the gelatinous zooplankton community sampled with the MultiNets was significantly impacted by the Chlorophyll a stock, the total mesozooplankton and macrozooplankton biomass, the percentage of AW and the latitude (Table 4).

Table 4 – P-values of the different environmental factors from the MIK net and MultiNet redundancy analysis. One star (*) or two stars (**) indicate respectively a p-value smaller than 0.05 or 0.01, hence show significant effect. A dot (.) indicates a p-value under 0.1 and shows possible effect.

Environmental factors	P-values from MIK net redundancy analysis	P-values from MultiNet redundancy analysis
AW percentage	0.1631	0.0037 (**)
Latitude	0.2000	0.0473 (*)
Total mesozooplankton and macrozooplankton biomass	0.0257 (*)	0.0317 (*)
Chlorophyll a stock	0.0023 (**)	0.0471 (*)
PW percentage	0.3323	0.4049
wPW percentage	0.7898	0.2686
Day of the year	0.2893	0.0868 (.)
Dinoflagellates and ciliates biomass	Not included	0.1446

In the MIK net redundancy analysis biplot (Figure 12A), the abundances of *Ptychogena lactea*, B*ougainvillia superciliaris, Euphysa flammea*, and *Mertensia ovum* were correlated to the percentage of wPW and total mesozooplankton and macrozooplankton biomass. *Sarsia* sp. and *Beroe* spp. were correlated to the chlorophyll a stock. *Aglantha digitale*, on the other hand, was correlated to the latitude, the day of the year, the number of water mass and the percentage of AW.

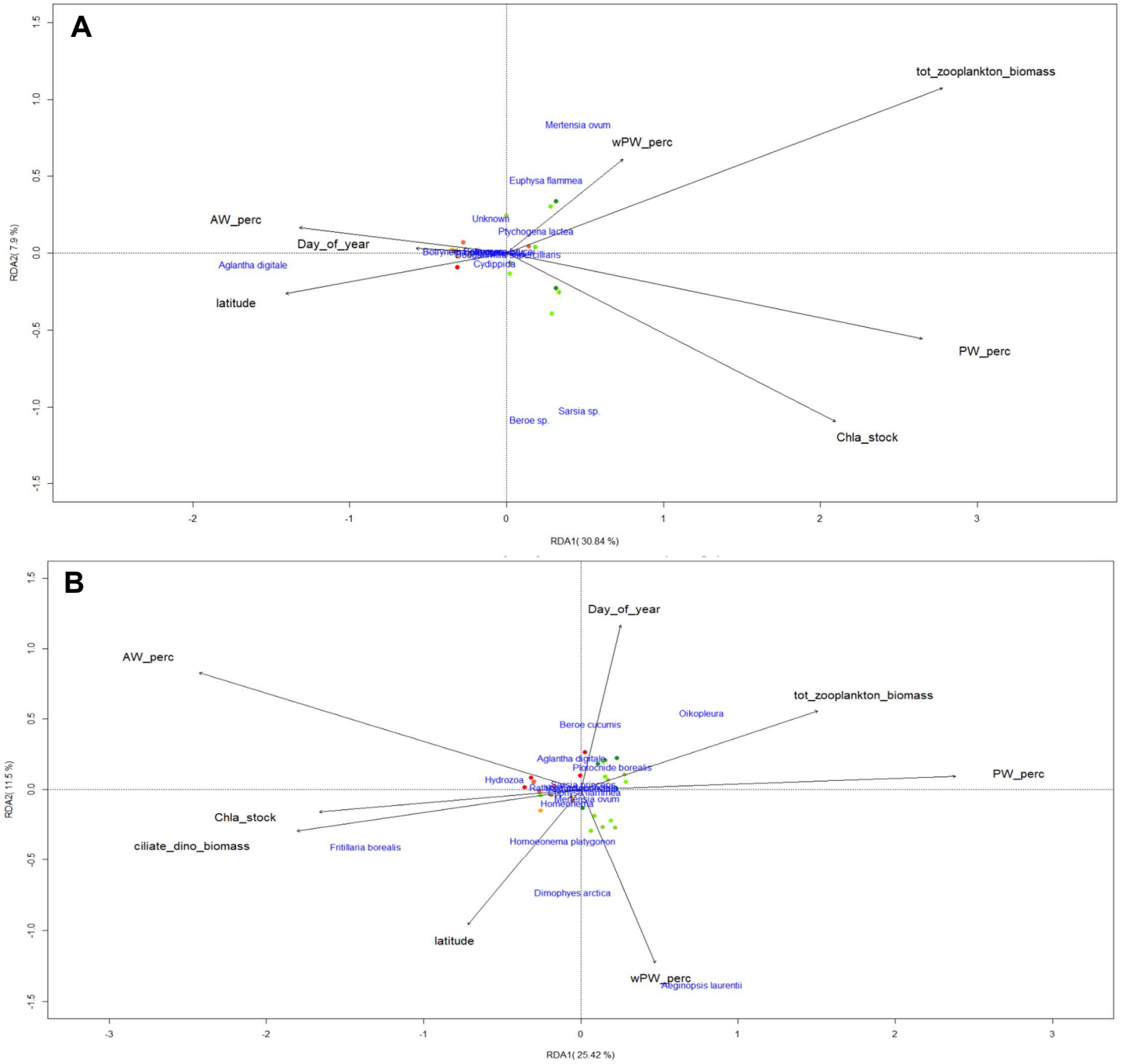

*Figure 12 - MIK net (**A**) and MultiNet (**B**) redundancy analysis biplot showing correlations between the gelatinous zooplankton taxa and the environmental factors*

In the MultiNet redundancy analysis biplot (Figure 12B), the abundance of *Fritillaria borealis* was correlated to the ciliates and dinoflagellates biomass, the chlorophyll a stock, the latitude and the percentage of AW. Similarly, the hydrozoa larvae abundance was correlated to the chlorophyll a stock and the percentage of AW. Differently, *Oikopleura sp*. and *Plotocnide borealis* were correlated to the total zooplankton biomass, the day of the year and the percentage

of PW. *Aeginopsis laurentii*, was correlated to the percentage of wPW. *Dimophyes arctica* and *Homoeonema platygonon* were also both correlated to the percentage of wPW and the latitude. Finally, *Aglantha digitale* and *Beroe cucumis*, were correlated with the day of the year.

3.6 *Beroe* genus identification and seasonal and distribution patterns

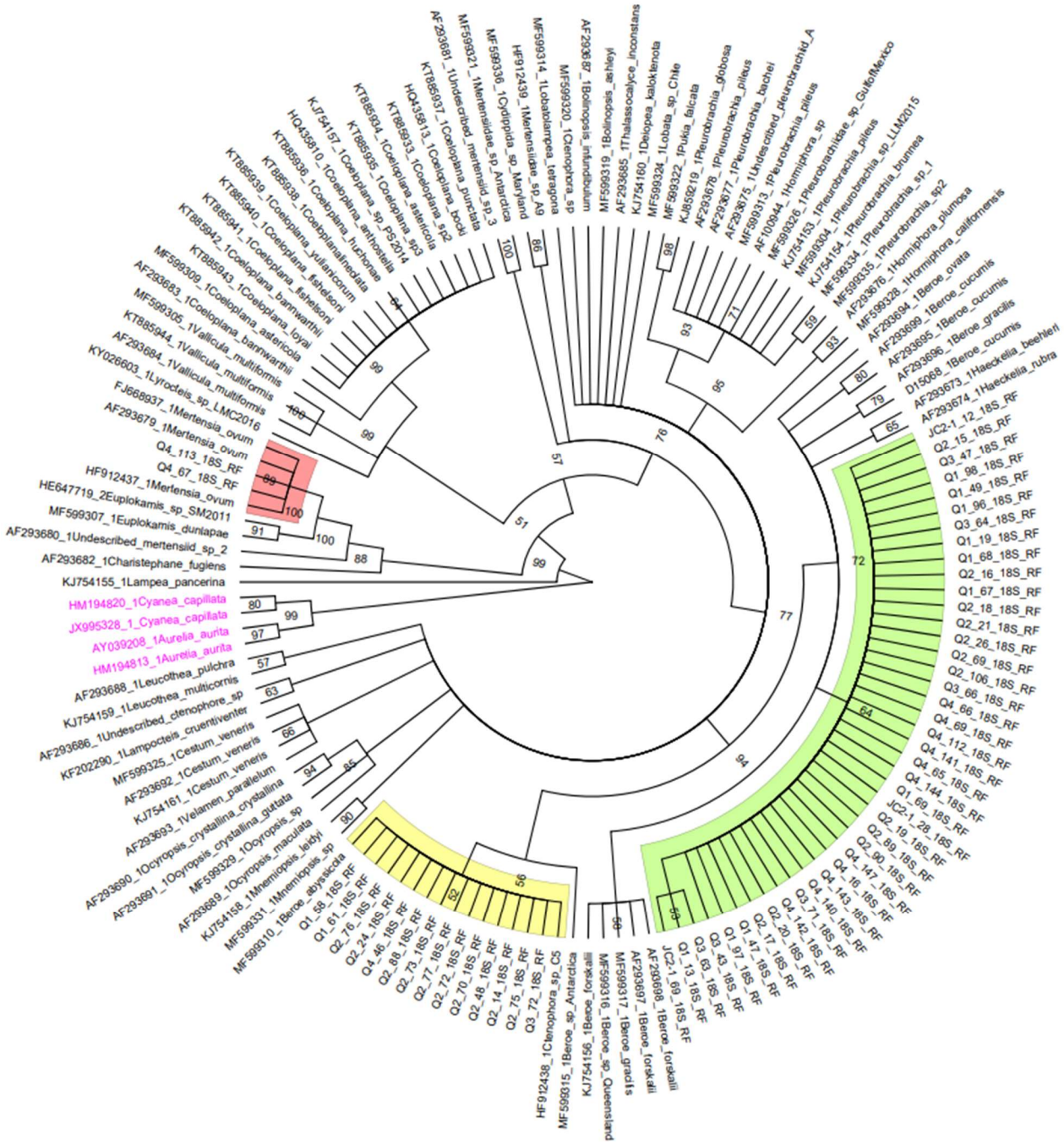

Figure 13 – 18S rRNA maximum likelihood (GTR+G+I model) phylogenetic tree, made with 141 Ctenophora sequences and four root sequences (pink). Bootstrap support values are located near their respective clade node and my sequences are grouped inside the coloured clade (green, yellow and red).

3.6.1 *Beroe* genus identification

The 58 *Beroe* spp. sequences from this study nested into three clades of the phylogenetic tree (Highlighted in green, yellow and red in the figure 13). The green clade included 42 of my *Beroe* spp. sequences, it was supported by a bootstrap value of 72%. Due to morphological characteristics matching with *Beroe Cucumis*, this clade was identified as *Beroe* cf. *cucumis*.

The yellow clade included 14 of my sequences and a *Beroe abyssicola* sequence from Genbank (MF599310). This clade was supported by a bootstrap value of 52%. The second higher clade was supported by bootstrap value of 94% and included one more unidentified *Beroe* spp. sequence from GenBank (HF912438). The sequences belonging to this second higher clade including the yellow clade were identified as *Beroe abyssicola.*

The red clade was well supported by bootstrap value of 89% and was composed of two of my sequences and three *Mertensia ovum* sequences from GenBank (FJ668937, AF293679, HF912437). The associated samples to my sequences were morphologically identified to *Beroe* spp. on board of the cruise. But considering their grouping with *Mertensia ovum* sequences and the high bootstrap value of the clade, they will be in the rest of my study identified as *M. ovum*.

3.6.2 *Beroe* genus distribution and seasonal patterns

Out of the two species belonging to the genus *Beroe, Beroe* cf. *cucumis* seemed more commonly detected in the study area and it was detected 15 times out of 28 sampling events. The highest number of *Beroe* cf. *cucumis* detected, was in the central Barents Sea in December with 6 individuals found (Figure 14B).

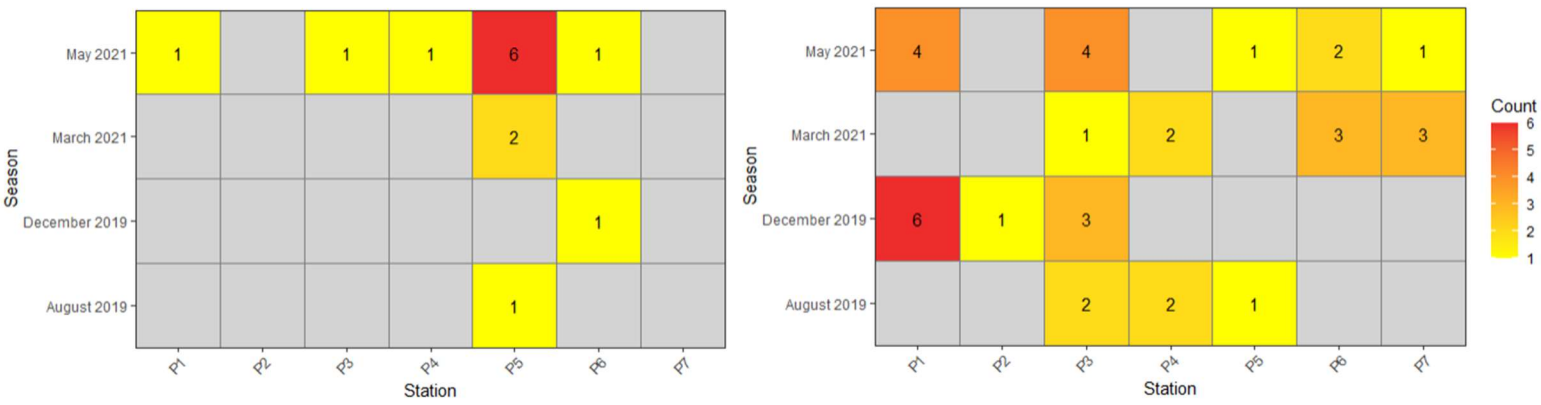

*Figure 14 – Number of Beroe abyssicola (**A**) and Beroe cf. cucumis (**B**) found along the transect (P1-P7) in August 2019, December 2019, March 2021 and May 2021. The color range from one individual (yellow) to six individuals (red) found. Grey is used when no individual was found.*

Beroe abyssicola, on the other hand, was more rarely detected in the study area and it was detected only 8 times out of 28 sampling events. It peaked in number in the northwest Barents Sea shelf station P5 in May with 6 individuals found (Figure 14A).

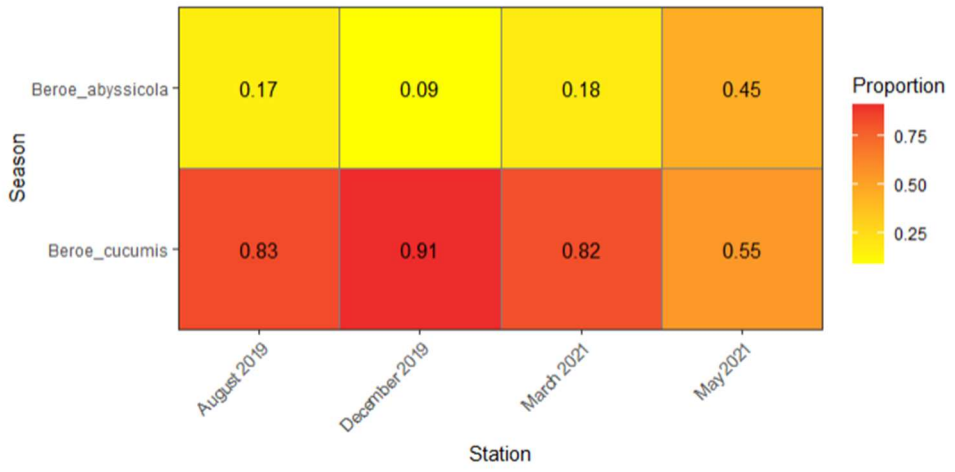

Figure 15 – Proportion of both species Beroe cf. cucumis and Beroe abyssicola in the study area in August 2019, December 2019, March 2021 and May 2021. The gradient of color illustrate the degree of dominance (yellow – dominated, red – dominant).

In the study area, the *Beroe* community was dominated by *Beroe* cf. *cucumis* from August to March with more than 82% of the *Beroe* spp. identified being *Beroe* cf. *cucumis* (Figure 15). Differently, in May, it was equally composed of *Beroe* cf. *cucumis* and *Beroe abyssicola* and when looking at the detail per station *Beroe abyssicola* dominated in the station P5 in May (Figure 15).

4 Discussion

Over the whole study area, including the central Barents Sea, the northwest Barents Sea and the Nansen Basin in the Arctic Ocean, 31 gelatinous zooplankton taxa were recorded. The most common and abundant taxa were, *Aglantha digitale*, *Beroe* spp., *Mertensia ovum*, *Dimophyes arctica*, *Oikopleura* sp., *Aeginopsis laurentii*, *Plotocnide borealis*, *Homoeonema platygonon*, *Sarsia* sp. and *Fritillaria borealis* (Figure 9, Appendix 8). Dvorestsky and Dvoretsky (2010) previously categorized most of these species as common in the Barents Sea, except the species *Dimophyes arctica* and *Homoeonema platygonon*. In my study, these two species were associated with PW and wPW, two widely advected water masses over the northern Barents Sea, hence possibly explaining why they were commonly present in the study area (Figure 1 & 12B). Additionally, some less abundant and rarely recorded taxa were found, notably, *Catablema vescicarium*, *Ptychogena lactea*, *Halitholus cirratus*, *Cyanea capillata*, *Dryodora glandiformis*, *Bougainvillia superciliaris*, *Euphysa flammea*, *Atolla tenella*, *Botrynema brucei*, *Botrynema ellinorae* and an unamed cydippid (Appendix 10, Figure 8 & 9).

Over the Barents Sea shelf, the meroplanktonic species *Rathkea octopunctata*, *Plotocnide borealis* and *Sarsia princeps*, were found in high abundance and the meroplanktonic species *Sarsia tubulosa*, *Ptychogena lactea*, *Bougainvillia supercilliaris* and *Halitholus cirratus,* were sometimes detected with low numbers (Figure 9, Appendix 10)(Ronowicz et al., 2015). These meroplanktonic species have been recorded several times before in the Barents Sea (Dvoretsky & Dvoretsky, 2010; Mańko et al., 2015; Zelickman, 1972). However, their distribution differed between areas in the Barents Sea, e.g. *Bougainvillia supercilliaris* was found in high numbers (11.48 ind.m^{-3}) in the Barents Sea Opening whereas in my study it was found in low numbers (Manko et al. 2015). In the literature, it has been shown, that due to the short life span of the medusae life stages, the abundances of the adult Cnidaria medusae population depend highly on the local polyp populations (Lucas et al., 2012). Hence, the differences in abundance, I observed between my study, Manko et al (2015) and Zelickman (1972) may reflect different polyp colonies repartition between the different regions of the Barents Sea. In my study area, the species *Rathkea octopunctata*, *Plotocnide borealis* and *Sarsia princeps* may then have numerous polyp colonies. However, in the Barents Sea, polyp colonies and their repartition have been understudied, hence I cannot check the veracity of my observations (Ronowicz et al., 2015). Arguably, the differences observed could also be due to interannual variability, seasonality or sampling biases due to patchiness (Eriksen et al., 2012; George, 1981; Yaragina et al., 2021).

Off the Barents Sea shelf, on the Barents Sea continental slope and in the Nansen Basin, respectively 900 meters and 3300 meters deep, the taxa *Atolla tenella*, *Botrynema ellinorae*, *Botrynema brucei*, *Sminthea eurygaster* and an unnamed cydippid were recorded in low numbers (Appendix 10). The unnamed cydippid was similar to the previously reported and referred "horned" cydippid or "ctenoceros" (Hosia & Båmstedt, 2007; Johnsen, 2005; Lindsay & Hunt, 2005). *Atolla tenella*, *Botrynema ellinorae*, *Botrynema brucei* and unnamed cydippid have been documented to live in deeper waters in the Amerasian Arctic Basin, across the Lomonosov Ridge and in the Fram Strait (Kosobokova & Hirche, 2000; Pantiukhin et al., 2023; K. A. Raskoff et al., 2005, 2010). Their occurrence in my study, in the Nansen Basin and Barents Sea continental slope consolidate that they are commonly distributed species in the Arctic Ocean. The taxa *Sminthea eurygaster* was to my knowledge for a first time recorded in the Arctic, and was notably found before in the Australian Waters and Adriatic Sea (Benović et al., 2005; Blackburn, 1955). As it was only detected on the continental slope and in the Nansen Basin, it may inhabit the deep waters (Appendix 10).

4.1 Environmental drivers of the gelatinous zooplankton community

The MIK net and MultiNet redundancy analysis conducted in my study showed that the gelatinous zooplankton community in the central Barents Sea, northern Barents Sea and Nansen Basin was significantly influenced by environmental factors (Table 4).

The primary production and the total zooplankton biomass had high spatio-temporal variations in the study area especially in the AW influenced areas (Figure 7). The primary production peaked in May and August due to the increasing light regime, stratification and sea ice retreat (Figure 7A)(Rey, 1985). It was higher in the AW influenced central Barents Sea and continental slope likely due to the replenishment of nutrient brought with the AW (Rey, 1985). The mesozooplankton and macrozooplankton biomass, peaked in August and December and was higher in the PW influenced northwest Barents Sea (Figure 7C). The primary production and zooplankton biomass have been reported before to highly impact gelatinous zooplankton communities, distribution and seasonality due to their direct effect on trophic interactions and life cycles (Deibel & Lowen, 2012; Kremer & Reeve, 1989; Lucas et al., 2014; Thein et al., 2013). Indeed, different gelatinous zooplankton taxa have different feeding behaviours and capture abilities leading to prey selections and as a result their repartition and abundance are

often closely related to their prey concentrations (Greene et al., 1986; Hansson & Kiørboe, 2006; Paley & Beemer, 2021). Prey availability has been shown in multiple studies to regulate spawning and reproduction of some taxa within the gelatinous phylum Appendicularia, Ctenophora and Cnidaria, hence, greatly impacting their timing of reproduction and seasonality (Deibel & Lowen, 2012; Kremer & Reeve, 1989; Thein et al., 2013).

The gelatinous zooplankton community was also significantly influenced by the influx of AW (Table 4). In my study area, AW was advected in the central Barents Sea and under the PW and wPW layers on the continental slope and in the Nansen Basin, cohering with previous studies in the region (Lind & Ingvaldsen, 2012; Loeng, 1991). In addition to influencing the Barents Sea temperatures, the advected AW also carry along expatriate zooplankton from the Atlantic Ocean and the Norwegian Sea (Ådlandsvik & Loeng, 1991; Hop et al., 2021; Lind & Ingvaldsen, 2012; Mańko et al., 2020). The AW expatriate species *Aglantha digitale* and *Fritillaria borealis* documented by Mańko et al (2015, 2020) and Blachowiak-Samolyk (2008) were also found and associated with AW in my study (Figure 12). However, they sometimes reached relatively high abundances in PW and wPW where no AW was advected, hence may not always be AW expatriates in the central and northwest Barents Sea (Figure 6, Appendix 9).

Finally, the gelatinous zooplankton community was also significantly influenced by the latitudes (Table 4). Indicating possible differences in the gelatinous zooplankton on the Barents Sea shelf and in the Arctic Ocean. Several studies documented before different zooplankton communities in the Arctic Ocean and the Shelf Seas (Abe et al., 2020; Ershova & Kosobokova, 2019). They were explained by multiple factors and notably because the Arctic Ocean is deeper, have stronger stratification and different light regimes due to the sea ice directly impacting the primary production dynamics (Tremblay et al., 2011). Additionally, polyp colonies repartition might change with greater depths (Ishii & Katsukoshi, 2010). In my study, the meroplanktonic gelatinous taxa were mostly reported on the Barents Sea shelf (see previous part) and rarely recorded in the Arctic Ocean, hence it might indicate less abundance of polyp colonies in the Arctic Ocean (Appendix 10). The differences I observed, may also be due to the unbalanced sampling as only one station was in the Arctic Ocean (P7).

It's important mentioning that, in both the MIK net and MultiNet redundancy analysis the unexplained variation was high and respectively of 50% and 52%. This could have been caused by a missing environmental factor in my analysis, for example the dissolved oxygen. Which was documented by Lucas et al (2014) to have significant impact on the gelatinous

zooplankton community. However, the high unexplained variation could also just indicate that the gelatinous zooplankton community was sometimes not impacted by external environmental factors.

4.2 Gelatinous zooplankton diversity patterns

The Arctic Ocean has relatively low diversity compared to other marine ecosystems (Gradinger et al., 2010). However, in my study the gelatinous zooplankton community with the highest and seasonally stable diversity was in the Nansen Basin due to the presence all year around of deep-water species and more widely distributed taxa (Figure 10, Appendix 10). The Nansen Basin due to its depth, has an important pressure gradient and with the presence of several water masses, it may have a high number of ecological niches, allowing a rich and diverse gelatinous zooplankton community (Figure 6). Moreover, the advection of Atlantic Water in the Nansen also caries species from further south into the Nansen basin, e.g. *Aglantha digitale*.

The gelatinous zooplankton community with the second highest and seasonally stable diversity was in the northwest Barents Sea in the PW/wPW influenced station P4, due to the presence of several meroplanktonic species, in addition to the commonly distributed taxa (Figure 4 & Figure 10).

Manko et al (2020) in the Fram Strait region, reported similar species to my study and documented also higher gelatinous diversity in colder Arctic Waters influenced shelf and deep areas compared to AW influenced areas. However, Manko et al (2015), also compared the diversity between the AW influenced areas PW influenced areas in the Barents Sea, and they found higher diversities in the AW influenced areas. In their study, they used only one net to sample the gelatinous zooplankton community and they estimated the diversity (species richness) with the number of taxa detected, which may have been a poor estimator of the diversity as the gelatinous zooplankton assemblage in the Barents Sea is diverse with many rarely recorded taxa (see above)(Chao & Chiu, 2016; Dvoretsky & Dvoretsky, 2010). Indeed, in theory the number of taxa detected converge toward the true species richness with increasing sampling effort (Chao & Chiu, 2016). But if the assemblage is diverse and with many rare taxa the rate of increase will be slower requiring higher sampling effort to estimate correctly the species richness (Chao & Chiu, 2016). Hence, using only one net per station and no replicates might not have been enough in their study to estimate the species/taxonomic richness with the

number of taxa detected, leading to random variations between stations. In my study, two different nets (MIK net and MultiNet) were used to sample the gelatinous zooplankton community possibly giving a better estimate of its diversity.

The gelatinous zooplankton diversity in the AW influenced central Barents Sea and continental slope was sometimes relatively high but it was highly variable between the seasons and was impacted by seasonal spawning of meroplanktonic species and changes in advections of wPW (Figure 6 & 10, Appendix 10). Indeed, with events of advections of wPW in the central Barents Sea some wPW associated taxa were found and notably *Aeginopsis laurentii* (Figure 12B).

4.3 Gelatinous zooplankton spatio-temporal dynamics

The highest gelatinous zooplankton abundances were reached in August, in the AW influenced stations, of which the central Barents Sea, had the highest gelatinous zooplankton abundance (Figure 9). This again cohere with previous results from Manko et al (2020) which reported in the Fram Strait higher abundances on the shelf and in the Atlantic Water influenced areas.

In my study, the seasonal peaks in abundance of the gelatinous zooplankton were tightly linked with peaks in primary production and zooplankton biomasses in accordance with previous studies (Figure 7 & 9, Table 4)(Bandara et al., 2016; Larson, 1986). In my study, the AW and PW influenced areas due to differences in their prey availability spatio-temporal dynamics had different gelatinous zooplankton community composition and seasonal dynamics.

4.3.1 Gelatinous zooplankton community seasonal dynamics in the AW influenced Central Barents Sea and Continental Slope

The central Barents Sea and Barents Sea continental slope were highly influenced by AW. They had due to the inflow of AW and its mixing with Barents Sea waters, high seasonal increases in primary production and secondary production in May and August (Ellingsen et al., 2008; Makarevich et al., 2012). The gelatinous zooplankton community was significantly influenced by the AW inflow and the gelatinous zooplankton total abundances highly increased in August coinciding with the peak in production and increase in temperatures (Figure 7 & 9 &

12). This is similar to previous studies at higher latitudes (Falkenhaug, 1996; Hosia & Båmstedt, 2007; Larson, 1986; Pertsova et al., 2006).

In May and August, the gelatinous zooplankton community was dominated by the two opportunistic feeder, *Fritillaria borealis and Oikopleura* sp., two appendicularians that have been reported to feed on phytoplankton and microzooplankton (Deibel & Turner, 1985). They both reached very high abundances in August (e.g 700 ind.m^{-3} and 120 ind.m^{-3}) in the euphotic zone above 100m depth, and sometimes at the interface between wPW and AW (Figure 6, Appendix 9). Hence, they may have contributed to a top-down control on the phytoplankton bloom. These appendicularians are known to be clutch size manipulators and have shorter generation times when the food availability and temperatures increase (Deibel & Lowen, 2012). Warmer temperatures due to the inflow of AW and the high concentration of phytoplankton and microzooplankton may have induced mass reproduction and occurrence of *Fritillaria borealis* and *Oikopleura sp*. in August in the central Barents Sea and Barents Sea continental slope. Simultaneously in May and August, numerous Hydrozoan larvae were found in the central Barents Sea and the Barents Sea continental slope up to 200m (Appendix 9). The high primary production and higher prey availabilities may have induced sexual reproduction of Hydrozoans (Figure 7 & 12). Indeed, Cnidaria sexual reproduction is often influenced by food availability as it requires high energy investments and because the reproductive success rates will depend on the amount of food ingested (Rossi et al., 2019). Also, as more Hydrozoan larvae were found in the warmer central Barents Sea, reproduction rates may have been higher with higher temperatures (Figure 11)(Rossi et al., 2019).

In December and March, the gelatinous zooplankton community abundances decreased sharply and the community composition was more mixed sometimes dominated by the carnivores species *Beroe* spp. and *Aglantha digitale*, and sometimes by the opportunistic feeder species *Fritillaria borealis* and *Oikopleura* sp. (Figure 9)(Deibel & Turner, 1985; Kamsilov, 1960; Pagès et al., 1996). The sharp drop in gelatinous zooplankton abundances from August to December may have been induced by the reduction of the reproduction rates with the sharp decrease in all prey biomasses and the high mortality of the short lived appendicularians *Oikopleura sp.* and *Fritillaria borealis*, which live only some weeks (Figure 7)(Alldredge, 1982; Deibel & Lowen, 2012). Due to these very low abundances in December and March, the differences found in the gelatinous zooplankton community composition are based on a small number of individuals and may come from local variations and patchiness.

The meroplanktonic species *Plotocnide borealis* and *Rathkea octopunctata* peaked in the central Barents Sea in May and August respectively (Figure 11). These seasonal peaks in abundance may have been initiated by a seasonal spawning event from polyp colonies and it may have been induced similarly to other Cnidaria taxa, by the seasonal warming of the water column with solar radiations and the seasonal increase in prey biomasses and light regimes (Lucas et al., 2012; Pertsova et al., 2006; Purcell et al., 2009; Thein et al., 2013). Zelickman (1972) also found in the Barents Sea that *Rathkea octopunctata* bud-off (spawning) from the polyp colonies happened in July, cohering with my observation.

4.3.2 Gelatinous zooplankton community seasonal dynamics in the northwest Barents Sea Shelf

The northwest Barents Sea shelf was highly influenced by PW and wPW. The primary production and microzooplankton biomass increased seasonally in May and August and the mesozooplankton and macrozooplankton biomass increased in August and December (Figure 7). The gelatinous zooplankton community total abundance peaked in August and December coinciding with the high primary production in August or the peak in mesozooplankton and macrozooplankton biomass in December (Figure 7 & 9).

In August, the gelatinous zooplankton community was similarly to the AW influenced areas dominated by the opportunistic feeders *Oikopleura* sp. and *Fritillaria borealis* (Figure 9)(Deibel & Turner, 1985). However, *Fritillaria borealis* reached lower abundances than in the AW influenced areas, possibly caused by the lower temperatures leading to slower reproduction rates and smaller clutch sizes (Deibel & Lowen, 2012). The gelatinous zooplankton community in August peaked in abundance around 50 meters depth deeper than in the AW influenced area possibly coinciding with the July sub-surface chlorophyll maximum reported by Rey (1985) in PW influenced regions of the Barents Sea (Appendix 9).

In December and March, the gelatinous zooplankton total abundances peaked vertically from 50m to 200m depth (Appendix 9), possibly following other zooplankton (potential preys) repartitions (Hirche & Kosobokova, 2011) (Bandara et al., 2016). The gelatinous zooplankton community was diverse with the presence of several sometime abundant carnivorous taxa, notably *Aeginopsis laurentii*, *Beroe cucumis*, *Mertensia ovum*, *Aglantha digitale*, *Dimophyes arctica* and *Homoeonema platygonon* (Barry, 1974; Dunn, 2009; Pagès et al., 1996; Siferd & Conover, 1992). The high number of carnivores taxa in the gelatinous zooplankton community was probably due to the high mesozooplankton and macrozooplankton biomasses, their

potential preys (Barry, 1974; Kamsilov, 1960; Nelson et al., 2000; Pagès et al., 1996; Siferd & Conover, 1992; Swanberg & Båmstedt, 1991a). In addition, the taxa *Oikopleura* sp. was also very abundant in December, possibly due its opportunistic diet and its ability to feed on copepods faecal pellets (Sampei et al., 2009). In March, *Oikopleura* sp. decreased in abundance, possibly due to the reduction of faecal pellets production by copepods due to the low prey availabilities (Seuthe et al., 2007).

In May, the gelatinous zooplanton community, was dominated by Aeginopsis laurentii and still mainly composed of carnivore taxa, such as *Aeginopsis laurentii*, *Beroe* spp., *Homoeonema platygonon*, *Dimophyes arctica* and *Plotocnide borealis*, but the phytoplankton and microzooplankton associated/predators taxa hydrozoan larvae and *Fritillaria borealis* increased in abundance, probably due to the seasonal increase in primary production (Figure 7).

The most abundant carnivore and opportunistic feeder species found in winter and spring in the PW/wPW influenced northwest Barents Sea were reported to reproduce in the winter (e.g. *Dimophyes arctica*), multiple times per year (e.g. Aglantha digitale) or all year around, (e.g. *Beroe cucumis*, *Mertensia ovum*, *Aeginopsis laurentii* and *Oikopleura* sp.) (Deibel & Lowen, 2012; Ikeda & Imamura, 1996; Jaspers, 2015; Jaspers et al., 2015; Mańko et al., 2020; Pertsova et al., 2006; Zelickman, 1972). Hence, due to the high winter zooplankton biomasses they may have been able to reproduce in the winter, leading to their dominance in the gelatinous zooplankton community.

The meroplanktonic taxa *Sarsia* sp. and *Plotocnide borealis* respectively peaked in abundance in August and May (Figure 8 & 11). Again, similarly to the AW areas, this was possibly due to a seasonal spawning from polyp colonies which may have been induced by the increase in primary production and light regimes (Figure 7) (Lucas et al., 2012; Pertsova et al., 2006; Purcell et al., 2009; Thein et al., 2013).

4.4 Distribution patterns in different water masses

As in the previous part, the AW and PW influenced areas had quite different gelatinous zooplankton community composition and abundances. These differences could have been the combined results of the gelatinous zooplankton specialized diets, the different prey distribution and the physical properties of the water masses (Figure 12).

Indeed, the taxa *Oikopleura* sp., *Plotocnide borealis*, *Beroe* spp. and *Mertensia ovum* were found in high abundances in wPW and PW but were not restricted to these water masses and sometimes peaked in abundance in AW (Figure 6, Appendix 9). Hence, their association in the redundancy analyses with the PW and wPW (Figure 12) was probably due to their carnivorous or detritivorous diets and the high mesozooplankton and macrozooplankton biomass in the PW and wPW influenced areas. On the other hand, the taxa *Aeginopsis laurentii*, *Dimophyes arctica*, *Sarsia* spp. and *Homeonema platygonon* were found and peaking only in wPW and PW (Figure 6, Appendix 9). Their restriction and correlation in the redundancy analyses to PW and wPW may have been induced by physical constraints, preventing them to survive in AW (Zelickman, 1972). Several meroplanktonic taxa were detected only in the PW/wPW influenced northwest Barents Sea, notably, *Halitholus cirratus*, *Ptychogena lactea*, *Sarsia princeps*, *Sarsia tubulosa*, *Bougainvillia supercilliaris* (Appendix 10). These taxa may be cold and fresh water adapted, hence leaving only in PW and wPW. However, this spatial detection pattern could also be due to unbalanced sampling, as most of the shelf stations were PW/wPW influenced.

Differently, the taxa Hydrozoa larvae, *Aglantha digitale* and *Fritillaria borealis* were found in highest abundances in AW, but sometimes in lower abundances in PW and wPW (Figure 6, Appendix 9). Their association with AW in Figure 12 was probably the result of the higher temperatures, their microzooplanktivorous and phytoplanktivorous juvenile and adult diets and the high primary production and microzooplankton biomass in AW influenced areas (Deibel & Lowen, 2012; Deibel & Turner, 1985; Pagès et al., 1996; Pedersen & Smidt, 2000). These taxa have been previously documented in the area to be associated with AW in the literature cohering with my observations (Blachowiak-Samolyk, 2008; Mańko et al., 2015, 2020).

4.5 *Beroe* genus identification, distribution and seasonal trends

4.5.1 *Beroe* genus identification

The *Beroe* spp. sequences in the green clade, morphologically identifies as *Beroe* cf. *cucumis* were nesting with several *Beroe* species and the clades were poorly supported. This illustrates the known complexity and problematics of the identification within the *Beroe* genus (Johansson et al., 2018; Shiganova & Abyzova, 2022). In my study area, Johansson et al (2018)

documented potential cryptic species in the *Beroe* genus and using DNA barcoding methods reported the presence of two new genetic lineage, *Beroe "norvegica"* and *Beroe "anatoliensis*" in addition to the previously reported species *Beroe cucumis* Fabricius 1780*, Beroe ovata* Mayer 1912 and *Beroe gracilis* Künne 1939. The lineage *Beroe "norvegica"* was later refuted by Shiganova and Abyzova (2021), which proposed that *Beroe "norvegica"* is in fact *Beroe cucumis* in polar regions and *Beroe cucumis* in subtropical, tropical and equatorial regions is *Beroe pseudocucumis*. My sequences did not group with *Beroe cucumis* sequences from Podar et al (2001) probably because their *Beroe cucumis* samples came from sub-tropical regions of the Atlantic Ocean (Santa Barbara and Florida, USA) and may not have been *Beroe cucumis,* Fabricius 1780. Indeed, the recent study Shiganova and Abyzova (2022) documented that *Beroe cucumis* in subtropical, tropical and equatorial regions of the Atlantic Ocean may be another specie, called *Beroe pseudocucumis.* Thus, illustrating the complexity and unsettled identification and phylogeny of the *Beroe* species.

The complexity in the identification and phylogeny of the *Beroe* genus is due to both the difficult morphological identifications and the absence of proper DNA barcoding protocols and reference libraries. Indeed, the common, universal cytochrome-c-oxidase subunit 1 (COI) primers do not work properly for ctenophores and the 18S marker is highly conservative and do not necessarily yield the resolution necessary for species level identification (Jucker & Havermans, 2022; Ortman, 2008; Podar et al., 2001). This, however, might change in the future with the use of different primers and markers as suggested by Christianson et al. (2021) and Jucker and Havermans (2022). *Beroe* species morphological identification can be difficult for someone untrained, as specific and difficult to observe taxonomic features should be investigated for example, the diverticules branching to the paragastric canals (Mills & Haddock, 2007). Additionally, when conserved *Beroe* specimens sometimes lose their diverticules, become opaque, shrink and lose their overall shape making the morphological identification impossible (Appendix 11). Morphological identification of *Beroe* species should then be done on fresh animals in order to see all taxonomic features needed for identification, a considerable constraint, considering the lack in sampling expedition of trained personnel able to identify *Beroe* species. However, different *Beroe* species may have different role in the Arctic foodweb and in order to estimate their present and future importance in the Arctic ecosystem consistent identification should be a priority.

4.5.2 *Beroe* genus distribution and seasonal trends

Beroe cf. *cucumis* was commonly found in my study area and is also commonly reported in the Barents Sea and Southern Barents Sea, which is probably due to its ability to reproduce all year around (Figure 14B, Appendix 10)(Mańko et al., 2015)(Dvorestsky and Dvoretsky 2010; Zelickman 1972) . Previous studies have reported *Beroe cucumis* to peak in abundance between May and August in the Barents Sea – Svalbard region, and to live mainly in the surface water in summer while sinking deeper in the winter (Bandara et al., 2016; Siferd & Conover, 1992; Swanberg & Båmstedt, 1991a; Zelickman, 1972). However, in my study I did not see any change in vertical position between the seasons, it was found throughout the water column up to 300m depth and peaked in abundances from December to March (Figure 11, Appendix 9). Such differences may have been related to the diet seasonal patterns discussed previously.

In my study, *Beroe abyssicola*, was rarely found and peaked in numbers in the PW influenced northwest Barents Sea shelf station P5 in May. *Beroe abyssicola* is a deep-water species, mainly living from 200 to 350 meters depth, but has been reported to survive also at shallower depths (Mackie, 1985; Mills & Haddock, 2007). Explaining why it could also be found in the shallow station P5 having a bottom depth of 160 meters. *Beroe abyssicola* has been recorded only very few times in the Global Biodiversity Information Facility (GBIF) in the Barents Sea, indicating that *Beroe abyssicola* may be rare in the Barents Sea (GBIF Secretariat, 2022). However, it is also likely that the few records in the Barents Sea are due to it being overlooked and difficult to be identify. *Beroe abyssicola* on GBIF was more often recorded in British Columbia and peaked in number of records in April, which is similar to my observation (Figure 14A) (GBIF Secretariat, 2022). Hence, the seasonal increase in number of *Beroe abyssicola* in May in the Barents Sea was possibly due to reproduction. However, as this based on few numbers, it should be regarded carefully.

Beroe abyssicola and *Beroe cucumis* are both chemokinetic search carnivores feeding on other ctenophores, but they may have different diets as suggested by Tamm and Tamm (1993) which described different macrociliary patterns between these two species (Swanberg, 1974). Macrocilia are finger-shaped, compound ciliary organelles found in the mouth of beroide ctenophores and are used for feeding (Horridge, 1965; Tamm & Tamm, 1993). Dissimilarities in the diets of the *Beroe cucumis and Beroe abyssicola* were confirmed in feeding studies (Paley & Beemer, 2021; Swanberg, 1974). Indeed, in Paley and Beemer (2021), *Beroe abyssicola* was able to feed only on *Bolinopsis infundibulum* and was not able to feed on *Pleurobrachia* sp.

possibly due to the lack of chemical trigger. *Beroe cucumis* on the other hand, was proven in several studies to feed on multiple ctenophores, such as *Mertensia ovum, Bolinopsis infundibulum*, *Pleurobrachia pileus*, and Swanberg (1974) reported that *Beroe cucumis* would eat any ctenophores they encounter (Anderson, 1974; Greve, 1970; Siferd & Conover, 1992; Swanberg, 1974). *Beroe cucumis* may then feed on a wider variety of preys that *Beroe abyssicola*. Hence, the seasonal changes in the dominance of the *Beroe* community I observed in Figure 15 may be accompanied with drastic changes in feeding dynamics and trophic interactions which should be investigated. For example, dominance of *Beroe abyssicola* instead of *Beroe cucumis* may lead to lower predation pressure on *Mertensia ovum* its assumed may prey in the Barents Sea, leading to an increase in their population and locally sharp decrease in their prey populations, notably copepods (Bandara et al., 2016; Majaneva, 2014; Majaneva et al., 2013; Swanberg & Båmstedt, 1991a, 1991b).

4.6 Method limitations

In this study, the collection of both physical and biological data over a full seasonal cycle allowed for a good review of the gelatinous zooplankton spatio-temporal dynamics. However, due to the one-year break in the sampling due to the COVID-19 pandemic, some of the differences observed may be linked to interannual variations instead of seasonal variations, especially considering the high interannual variability of the gelatinous zooplankton community in the Barents Sea (Yaragina et al., 2021; Zelickman, 1972). Decerning between interannual and seasonal variations was difficult to investigate because the years and seasons were not independent.

The use of both MIK nets and MultiNets for the gelatinous zooplankton data collection greatly increased the sampling coverage and coupled with the rechecking of the species identity with both morphological and molecular methods allowed a better assessment of the rarer taxa and diversity in the region. Even if, my estimations of the diversity can still be discussed as these two gears gave significantly different estimation of the gelatinous zooplankton community and may be adapted for different things. MIK nets caught larger individuals and were better to detect rarer taxa and deep-water species whereas the MultiNets were better to investigate vertical distributions and gave better abundance estimations. The MultiNet were also sensibly better to sample appendicularians. These differences should be considered in the future gelatinous zooplankton studies. Additionally due to their differences, they could not be

used as replicates and the variation within each station could not be identified and abundances patterns were sometimes based on a very low number of individuals. Future studies may need to include a true replicate in order to assess the patchiness, the variability within each stations and obtain strong abundance estimates (George, 1981). Especially, considering the aggregation and patchiness of gelatinous zooplankton (Graham et al., 2001).

Considering everything that was learned in this study, a potential study design to study the gelatinous zooplankton diversity, distribution and seasonality was developed. It can be found in Table 5.

Table 5 - Potential study design for a gelatinous zooplankton diversity, distribution and seasonality study

Study area and investigation period	Sampling area: The study area should be selected in order to reduce unwanted variations of the environmental factors, for example if the goal is to compare two oceanic domains, the best is to have the same number of stations between the two domains and to choose stations with similar depths. Sampling period: To study the gelatinous zooplankton spatio-temporal dynamics, a minimum of four surveys should be included in order to cover the full seasonal cycle. If possible, more than four cruise should be done, to reduce the probability of missing seasonal peaks in abundance/bloom events. Indeed, the life span of gelatinous zooplankton can range from a week (e.g. for Appendicularia) to some months (e.g. for Cnidarians medusae) and bloom events may not be sustained during long periods of times (Alldredge, 1982; Lucas et al., 2012).
Data collection	ROV: To get gelatinous zooplankton abundances with a high vertical resolution and *in situ* observations of their predation behaviours. Also, it does not underestimate fragile taxa and with long soak times, it's a good sampling gear to detect rarer taxa and deep-water species (Raskoff et al., 2010). Species identification can be limited due to the recording quality.

	MultiNet (64 and 180µm): To collect gelatinous zooplankton abundances and assess their vertical distribution. Good to sample the missed transparent taxa from the ROV, e.g. *Aglantha digitale* (Raskoff et al., 2005). CTD: To record the physical properties of the water column. Crucial to study the gelatinous zooplankton spatio-temporal dynamics, considering their tight relation with water masses (Mańko et al., 2015). Note: Regardless of what sampling chosen to collect the data, a standard and consistent protocol should be applied to reduce unwanted variability.
Identification	If possible, the identification should be done on board on the fresh individuals in order to avoid the loss of morphological features during the conservation (Appendix 11). If possible, take good quality pictures with scales of the fresh individuals for possible identity rechecking.
Conservation	The samples identified or not should be kept in >96% non-denatured EtOH at -20°C, for further identification, possible DNA barcoding and population genetics studies.

5 Conclusion

The aim of this master thesis was to (1) investigate diversity and distribution patterns between the different water masses and regions from the northern Barents Sea and (2) investigate the gelatinous zooplankton seasonality over a whole year in the northern Barents Sea. This was successfully done and I found that the gelatinous zooplankton community in the Northern Barents Sea was highly influenced by the primary production, the zooplankton biomasses, the latitudes and the advection of AW.

In the AW influenced central Barents Sea and continental slope, the gelatinous zooplankton community diversity and abundance changed highly with seasons. The total abundances peaked in August, coincidently with the high food availabilities and temperatures. The gelatinous zooplankton community was dominated by the opportunistic feeders/grazers, *Fritillaria borealis* and *Oikopleura sp.*.

In the PW/wPW influenced northwest Barents Sea, on the other hand, the gelatinous zooplankton community had relatively lower seasonal changes in diversity and abundance. The total abundances peaked in August or December coincidently with the high primary production or the high zooplankton biomasses. The PW/wPW gelatinous community differently to AW influenced areas changed seasonally and shifted over the winter from an opportunistic feeder community (dominated by *Oikopleura* sp.) to a carnivore community (dominated by *Aeginopsis laurentii*).

Futures changes, such as higher advection of AW may as a result lead to more seasonally variable communities, possibly leading to stronger grazing/predation events which may indirectly influence zooplankton stocks and higher trophic levels. Further justifying the need of standardized, consistent and coordinated monitoring of the gelatinous zooplankton communities in the Barents Sea.

References

Abe, Y., Matsuno, K., Fujiwara, A., & Yamaguchi, A. (2020). Review of spatial and inter-annual changes in the zooplankton community structure in the western Arctic Ocean during summers of 2008–2017. *Progress in Oceanography*, *186*, 102391. https://doi.org/10.1016/j.pocean.2020.102391

Ådlandsvik, B., & Loeng, H. (1991). A study of the climatic system in the Barents Sea. *Polar Research*, *10*(1), 45–50. https://doi.org/10.3402/polar.v10i1.6726

Agassiz, A. (1865). *Illustrated Catalogue of the Museum of Comparative Zoology: North American Acalephae*. Cambridge University Press.

Aksenov, Y., Ivanov, V. V., Nurser, A. J. G., Bacon, S., Polyakov, I. V., Coward, A. C., Naveira-Garabato, A. C., & Beszczynska-Moeller, A. (2011). The Arctic Circumpolar Boundary Current. *Journal of Geophysical Research: Oceans*, *116*(C9). https://doi.org/10.1029/2010JC006637

Alldredge, A. L. (1982). Aggregation of Spawning Appendicularians in Surface Windrows. *Bulletin of Marine Science*, *32*(1), 250–254.

Alldredge, A. L. (1984). The Quantitative Significance of Gelatinous Zooplankton as Pelagic Consumers. In M. J. R. Fasham (Ed.), *Flows of Energy and Materials in Marine Ecosystems: Theory and Practice* (pp. 407–433). Springer US.

Alvariño, A. (1985). *Predation in the plankton realm; mainly with reference to fish larvae*.

Anderson, E. (1974). *Trophic interactions among ctenophores and copepods in St. Margaret's Bay, Nova Scotia.*

Arai, M., Brodeur, R., Purcell, J., & Uye, S. (2017). *Physio-ecological properties of jellyfish*.

Asch, R. G., Stock, C. A., & Sarmiento, J. L. (2019). Climate change impacts on mismatches between phytoplankton blooms and fish spawning phenology. *Global Change Biology*, *25*(8), 2544–2559. https://doi.org/10.1111/gcb.14650

Bandara, K., Varpe, Ø., Søreide, J. E., Wallenschus, J., Berge, J., & Eiane, K. (2016). Seasonal vertical strategies in a high-Arctic coastal zooplankton community. *Marine Ecology Progress Series*, *555*, 49–64. https://doi.org/10.3354/meps11831

Barry, B. (1974). *Hydromedusae of the Canadian eastern Arctic*.

Barton, B. I., Lenn, Y.-D., & Lique, C. (2018). Observed Atlantification of the Barents Sea Causes the Polar Front to Limit the Expansion of Winter Sea Ice. *Journal of Physical Oceanography*, *48*(8), 1849–1866. https://doi.org/10.1175/JPO-D-18-0003.1

Benović, A., Lučić, D., Onofri, V., Batistić, M., & Njire, J. (2005). Bathymetric distribution of medusae in the open waters of the middle and south Adriatic Sea during spring 2002. *Journal of Plankton Research*, *27*(1), 79–89.

Blachowiak-Samolyk, K. (2008). Contrasting zooplankton communities (Arctic vs. Atlantic) in the European Arctic Marginal Ice Zone. *Oceanologia*, *50*(3), 363–389.

Blackburn, M. (1955). Trachymedusae and Narcomedusae of south-east Australian waters. *Marine and Freshwater Research*, *6*(3), 410–428.

Boero, F., Bouillon, J., Gravili, C., Miglietta, M., Parsons, T., & Piraino, S. (2008). Gelatinous plankton: Irregularities rule the world (sometimes). *Marine Ecology Progress Series*, *356*, 299–310. https://doi.org/10.3354/meps07368

Borcard, D., Gillet, F., & Legendre, P. (2011). *Numerical ecology with R* (Vol. 2). Springer.

Bouillon, J., Medel, M. D., Pagès, F., Gili, J. M., Boero, F., & Gravili, C. (2004). Fauna of the Mediterranean hydrozoa. *Scientia Marina*, *68*(S2), 5–438.

Brodeur, R. D., Ruzicka, J. J., & Steele, J. H. (2011). Investigating alternate trophic pathways through gelatinous zooplankton and planktivorous fishes in an upwelling ecosystem using end-to-end models. *Interdisciplinary Studies on Marine Environmental Modeling & Analysis*, 57–63.

Brodeur, R. D., Suchman, C. L., Reese, D. C., Miller, T. W., & Daly, E. A. (2008). Spatial overlap and trophic interactions between pelagic fish and large jellyfish in the northern California Current. *Marine Biology*, *154*, 649–659.

Chao, A., & Chiu, C.-H. (2016). *Species Richness: Estimation and Comparison* (pp. 1–26). https://doi.org/10.1002/9781118445112.stat03432.pub2

Collins, A. G. (2002). Phylogeny of Medusozoa and the evolution of cnidarian life cycles. *Journal of Evolutionary Biology*, *15*(3), 418–432.

Cornish-Bowden, A. (1985). Nomenclature for incompletely specified bases in nucleic acid sequences: Recommendations 1984. *Nucleic Acids Research*, *13*(9), 3021.

Deibel, D., & Lowen, B. (2012). A review of the life cycles and life-history adaptations of pelagic tunicates to environmental conditions. *ICES Journal of Marine Science*, *69*(3), 358–369. https://doi.org/10.1093/icesjms/fsr159

Deibel, D., & Turner, J. T. (1985). Zooplankton feeding ecology: Contents of fecal pellets of the appendicularian Oikopleura vanhoeffeni. *Marine Ecology Progress Series*, *27*(1/2), 67–78.

Drinkwater, K. F. (2011). The influence of climate variability and change on the ecosystems of the Barents Sea and adjacent waters: Review and synthesis of recent studies from the NESSAS Project. *Progress in Oceanography*, *90*(1), 47–61. https://doi.org/10.1016/j.pocean.2011.02.006

Dunn, C. (2009). Siphonophores. *Current Biology*, *19*(6), R233–R234.

Dvoretsky, V. G., & Dvoretsky, A. G. (2010). Checklist of fauna found in zooplankton samples from the Barents Sea. *Polar Biology*, *33*(7), 991–1005.

Edgar, A., Ponciano, J. M., & Martindale, M. Q. (2022). Ctenophores are direct developers that reproduce continuously beginning very early after hatching. *Proceedings of the National Academy of Sciences*, *119*(18), e2122052119.

Ellingsen, I. H., Dalpadado, P., Slagstad, D., & Loeng, H. (2008). Impact of climatic change on the biological production in the Barents Sea. *Climatic Change*, *87*(1), 155–175. https://doi.org/10.1007/s10584-007-9369-6

Eriksen, E., Benzik, A. N., Dolgov, A. V., Skjoldal, H. R., Vihtakari, M., Johannesen, E., Prokhorova, T. A., Keulder-Stenevik, F., Prokopchuk, I., & Strand, E. (2020). Diet and trophic structure of

fishes in the Barents Sea: The Norwegian-Russian program “year of stomachs” 2015–establishing a baseline. *Progress in Oceanography*, *183*, 102262.

Eriksen, E., Bogstad, B., Dolgov, A., & Beck, I. M. (2018). Cod diet as an indicator of Ctenophora abundance dynamics in the Barents Sea. *Marine Ecology Progress Series*, *591*, 87–100.

Eriksen, E., Gjøsæter, H., Prozorkevich, D., Shamray, E., Dolgov, A., Skern-Mauritzen, M., Stiansen, J. E., Kovalev, Yu., & Sunnanå, K. (2018). From single species surveys towards monitoring of the Barents Sea ecosystem. *Progress in Oceanography*, *166*, 4–14. https://doi.org/10.1016/j.pocean.2017.09.007

Eriksen, E., Prozorkevich, D., Trofimov, A., & Howell, D. (2012). Biomass of Scyphozoan Jellyfish, and Its Spatial Association with 0-Group Fish in the Barents Sea. *PLOS ONE*, *7*(3), e33050. https://doi.org/10.1371/journal.pone.0033050

Ershova, E. A., & Kosobokova, K. N. (2019). Cross-shelf structure and distribution of mesozooplankton communities in the East-Siberian Sea and the adjacent Arctic Ocean. *Polar Biology*, *42*(7), 1353–1367. https://doi.org/10.1007/s00300-019-02523-2

Falkenhaug, T. (1996). Distributional and seasonal patterns of ctenophores in Malangen, northern Norway. *Marine Ecology Progress Series*, *140*, 59–70.

Fossheim, M., Primicerio, R., Johannesen, E., Ingvaldsen, R. B., Aschan, M. M., & Dolgov, A. V. (2015). Recent warming leads to a rapid borealization of fish communities in the Arctic. *Nature Climate Change*, *5*(7), Article 7. https://doi.org/10.1038/nclimate2647

George, D. G. (1981). *Zooplankton patchiness*.

Gradinger, R., Bluhm, B. A., Hopcroft, R. R., Gebruk, A. V., Kosobokova, K., Sirenko, B., & Wesławski, J. M. (2010). Marine life in the Arctic. *Life in the World’s Oceans: Diversity, Distribution and Abundance. Wiley-Blackwell, Oxford*, 183–202.

Graham, W. M., Pagès, F., & Hamner, W. M. (2001). A physical context for gelatinous zooplankton aggregations: A review. In J. E. Purcell, W. M. Graham, & H. J. Dumont (Eds.), *Jellyfish Blooms: Ecological and Societal Importance* (pp. 199–212). Springer Netherlands. https://doi.org/10.1007/978-94-010-0722-1_16

Greene, C. H., Landry, M. R., & Monger, B. C. (1986). Foraging behavior and prey selection by the ambush entangling predator Pleurobrachia bachei. *Ecology*, *67*(6), 1493–1501.

Greve, W. (1970). Cultivation experiments on North Sea ctenophores. *Helgoländer Wissenschaftliche Meeresuntersuchungen*, *20*(1), 304–317.

Halsband, C., Majaneva, S., Hosia, A., Emaus, P. A., Gaardsted, F., Zhou, Q., Nøst, O. A., & Renaud, P. E. (2018). Jellyfish summer distribution, diversity and impact on fish farms in a Nordic fjord. *Marine Ecology Progress Series*, *591*, 267–279.

Hamilton, G. (2016). The secret lives of jellyfish: Long regarded as minor players in ocean ecology, jellyfish are actually important parts of the marine food web. *Nature*, *531*(7595), 432–435.

Hansson, L. J., & Kiørboe, T. (2006). Prey-specific encounter rates and handling efficiencies as causes of prey selectivity in ambush-feeding hydromedusae. *Limnology and Oceanography*, *51*(4), 1849–1858. https://doi.org/10.4319/lo.2006.51.4.1849

Harbison, L. M. G. (2009). Gelatinous zooplankton. *Elements of Physical Oceanography: A Derivative of the Encyclopedia of Ocean Sciences*, 51.

Hirche, H. J., & Kosobokova, K. N. (2011). Winter studies on zooplankton in Arctic seas: The Storfjord (Svalbard) and adjacent ice-covered Barents Sea. *Marine Biology*, *158*(10), 2359–2376. https://doi.org/10.1007/s00227-011-1740-5

Holthus, P., Clarkin, C., & Lorentzen, J. (2013). Emerging Arctic Opportunities: Dramatic increases expected in Arctic shipping, oil and gas exploration, fisheries, and tourism. *Coast Guard Journal of Safety & Security at Sea, Proceedings of the Marine Safety & Security Council*, *70*(2). https://trid.trb.org/view/1266079

Hop, H., Wold, A., Meyer, A., Bailey, A., Hatlebakk, M., Kwasniewski, S., Leopold, P., Kuklinski, P., & Søreide, J. E. (2021). Winter-Spring Development of the Zooplankton Community Below Sea Ice in the Arctic Ocean. *Frontiers in Marine Science*, *8*. https://doi.org/10.3389/fmars.2021.609480

Horridge, G. A. (1965). Macrocilia with numerous shafts from the lips of the ctenophore Beroe. *Proceedings of the Royal Society of London. Series B. Biological Sciences*, *162*(988), 351–364.

Hosia, A., & Båmstedt, U. (2007). Seasonal changes in the gelatinous zooplankton community and hydromedusa abundances in Korsfjord and Fanafjord, western Norway. *Marine Ecology Progress Series*, *351*, 113–127.

Hwang, S.-W., Kang, H.-K., Son, Y.-B., Jang, M.-C., & Choi, K.-H. (2013). Collapse of the Crustacean Mesozooplankton in the Northern East China Sea: Effects of the Three Gorges Dam? *Journal of Coastal Research*, *29*(6), 1464–1469. https://doi.org/10.2112/JCOASTRES-D-13-00011.1

Ikeda, T., & Imamura, A. (1996). Abundance, vertical distribution and life cycle of a hydromedusa Aglantha digitale in Toyama bay, southern Japan Sea. *Bulletin of Plankton Society of Japan (Japan)*. https://scholar.google.com/scholar_lookup?title=Abundance%2C+vertical+distribution+and+life+cycle+of+a+hydromedusa+Aglantha+digitale+in+Toyama+bay%2C+southern+Japan+Sea&author=Ikeda%2C+T.+%28Japan+Sea+National+Fisheries+Research+Inst.%2C+Niigata+%28Japan%29%29&publication_year=1996

Ishii, H., & Katsukoshi, K. (2010). Seasonal and vertical distribution of Aurelia aurita polyps on a pylon in the innermost part of Tokyo Bay. *Journal of Oceanography*, *66*(3), 329–336. https://doi.org/10.1007/s10872-010-0029-5

Jaspers, C. (2015). 2.7 Mertensia ovum (Fabricius, 1780), Sea nut. *BIO-C3 Biodiversity Changes: Causes, Consequences and Management Implications*, 41.

Jaspers, C., Acuña, J. L., & Brodeur, R. D. (2015). Interactions of gelatinous zooplankton within marine food webs. *Journal of Plankton Research*, *37*(5), 985–988. https://doi.org/10.1093/plankt/fbv068

Johansson, M., Shiganova, T., Ringvold, H., Stupnikova, A., Heath, D., & MacIsaac, H. (2018). Molecular Insights Into the Ctenophore Genus Beroe in Europe: New Species, Spreading Invaders. *The Journal of Heredity*, *109*. https://doi.org/10.1093/jhered/esy026

Johnsen, S. (2005). The Red and the Black: Bioluminescence and the Color of Animals in the Deep Sea1. *Integrative and Comparative Biology*, *45*(2), 234–246. https://doi.org/10.1093/icb/45.2.234

Jucker, M. N., & Havermans, C. (2022, September 13). The phylogeography of two Beroe species in the Arctic Ocean based on one mitochondrial and one ribosomal marker. *EPIC3ICYMARE International Conference for Young Marine Researchers, Bremerhaven, 2022-09-13-2022-09-16*. ICYMARE International Conference for Young Marine Researchers, Bremerhaven. https://epic.awi.de/id/eprint/57231/

Kamsilov, M. M. (1960). Nutrition of the ctenophore Beroe cucumis, Fabr. *Doklady Akademii Nauk SSSR*, *130*, 1138–1140.

Katoh, K., Misawa, K., Kuma, K., & Miyata, T. (2002). MAFFT: a novel method for rapid multiple sequence alignment based on fast Fourier transform. *Nucleic Acids Research*, *30*(14), 3059–3066.

Katoh, K., & Standley, D. M. (2013). MAFFT Multiple Sequence Alignment Software Version 7: Improvements in Performance and Usability. *Molecular Biology and Evolution*, *30*(4), 772–780. https://doi.org/10.1093/molbev/mst010

Kawahara, M., Uye, S., Ohtsu, K., & Iizumi, H. (2006). Unusual population explosion of the giant jellyfish Nemopilema nomurai (Scyphozoa: Rhizostomeae) in East Asian waters. *Marine Ecology-Progress Series - MAR ECOL-PROGR SER*, *307*, 161–173. https://doi.org/10.3354/meps307161

Kober, K. M., & Nichols, S. A. (2007). On the phylogenetic relationships of hadromerid and poecilosclerid sponges. *Journal of the Marine Biological Association of the United Kingdom*, *87*(6), 1585–1598.

Kosobokova, K., & Hirche, H.-J. (2000). Zooplankton distribution across the Lomonosov Ridge, Arctic Ocean: Species inventory, biomass and vertical structure. *Deep Sea Research Part I Oceanographic Research Papers*, *47*, 2029–2060. https://doi.org/10.1016/S0967-0637(00)00015-7

Kremer, P., & Reeve, M. R. (1989). Growth dynamics of a ctenophore (Mnemiopsis) in relation to variable food supply. II. Carbon budgets and growth model. *Journal of Plankton Research*, *11*(3), 553–574. https://doi.org/10.1093/plankt/11.3.553

Kvingedal, B. (2005). Sea-ice extent and variability in the Nordic Seas, 1967—2002. *Washington DC American Geophysical Union Geophysical Monograph Series*, *158*, 39–49.

Larson, R. J. (1986). Seasonal changes in the standing stocks, growth rates, and production rates of gelatinous predators in Saanich Inlet, British Columbia. *Marine Ecology Progress Series*, *33*, 89–98.

Legendre, P., & Gallagher, E. D. (2001). Ecologically meaningful transformations for ordination of species data. *Oecologia*, *129*, 271–280.

Legendre, P., & Legendre, L. (2012). *Numerical ecology*. Elsevier.

Licandro, P., & Lindsay, D. J. (2017). Ctenophora. *Oxford Scholarship Online*.

Lind, S., & Ingvaldsen, R. B. (2012). Variability and impacts of Atlantic Water entering the Barents Sea from the north. *Deep Sea Research Part I: Oceanographic Research Papers*, *62*, 70–88. https://doi.org/10.1016/j.dsr.2011.12.007

Lindsay, D. J., & Hunt, J. C. (2005). Biodiversity in midwater cnidarians and ctenophores: Submersible-based results from deep-water bays in the Japan Sea and north-western Pacific. *Journal of the Marine Biological Association of the United Kingdom*, *85*(3), 503–517.

Loeng, H. (1991). Features of the physical oceanographic conditions of the Barents Sea. *Polar Research*, *10*. https://doi.org/10.3402/polar.v10i1.6723

Loeng, H., Brander, K., Carmack, E., Denisenko, S., Drinkwater, K., Hansen, B., Kovacs, K., Livingston, P., McLaughlin, F., & Sakshaug, E. (2005). Marine systems. *Arctic Climate Impact Assessment*, *453538*.

Loeng, H., & Drinkwater, K. (2007). An overview of the ecosystems of the Barents and Norwegian Seas and their response to climate variability. *Deep Sea Research Part II: Topical Studies in Oceanography*, *54*(23), 2478–2500. https://doi.org/10.1016/j.dsr2.2007.08.013

Lucas, C. H., Graham, W. M., & Widmer, C. (2012). Chapter Three - Jellyfish Life Histories: Role of Polyps in Forming and Maintaining Scyphomedusa Populations. In M. Lesser (Ed.), *Advances in Marine Biology* (Vol. 63, pp. 133–196). Academic Press. https://doi.org/10.1016/B978-0-12-394282-1.00003-X

Lucas, C. H., Jones, D. O. B., Hollyhead, C. J., Condon, R. H., Duarte, C. M., Graham, W. M., Robinson, K. L., Pitt, K. A., Schildhauer, M., & Regetz, J. (2014). Gelatinous zooplankton biomass in the global oceans: Geographic variation and environmental drivers. *Global Ecology and Biogeography*, *23*(7), 701–714. https://doi.org/10.1111/geb.12169

Lynam, C. P., Gibbons, M. J., Axelsen, B. E., Sparks, C. A., Coetzee, J., Heywood, B. G., & Brierley, A. S. (2006). Jellyfish overtake fish in a heavily fished ecosystem. *Current Biology*, *16*(13), R492–R493.

Mackie, G. O. (1985). Midwater macroplankton of British Columbia studied by submersible PISCES IV. *Journal of Plankton Research*, *7*(6), 753–777. https://doi.org/10.1093/plankt/7.6.753

Madeira, F., Pearce, M., Tivey, A. R. N., Basutkar, P., Lee, J., Edbali, O., Madhusoodanan, N., Kolesnikov, A., & Lopez, R. (2022). Search and sequence analysis tools services from EMBL-EBI in 2022. *Nucleic Acids Research*, *50*(W1), W276–W279. https://doi.org/10.1093/nar/gkac240

Majaneva, S. (2014). *Understanding the biodiversity and ecological importance of ctenophores Lessons from Arctic and Baltic Mertensia ovum*. https://helda.helsinki.fi/handle/10138/43182

Majaneva, S., Berge, J., Renaud, P. E., Vader, A., Stübner, E., Rao, A. M., Sparre, Ø., & Lehtiniemi, M. (2013). Aggregations of predators and prey affect predation impact of the Arctic ctenophore Mertensia ovum. *Marine Ecology Progress Series*, *476*, 87–100. https://doi.org/10.3354/meps10143

Majaneva, S., & Majaneva, M. (2013). Cydippid ctenophores in the coastal waters of Svalbard: Is it only Mertensia ovum? *Polar Biology*, *36*(11), 1681–1686.

Makarevich, P., Druzhkova, E., & Larionov, V. (2012). Primary producers of the Barents Sea. *Diversity of Ecosystems*, 367–393.

Makoto, O., & Tsutomu, I. (1984). *Methods in marine zooplankton ecology.* https://scholar.google.com/scholar_lookup?title=Methods+in+marine+zooplankton+ecology.&author=Omori+Makoto&publication_year=1984

Mańko, M. K., Gluchowska, M., & Weydmann-Zwolicka, A. (2020). Footprints of Atlantification in the vertical distribution and diversity of gelatinous zooplankton in the Fram Strait (Arctic Ocean). *Progress in Oceanography*, *189*, 102414. https://doi.org/10.1016/j.pocean.2020.102414

Mańko, M. K., Panasiuk-Chodnicka, A. A., & Żmijewska, M. I. (2015). Pelagic coelenterates in the Atlantic sector of the Arctic Ocean − species diversity and distribution as water mass indicators. *Oceanological and Hydrobiological Studies*, *44*(4), 466–479. https://doi.org/doi:10.1515/ohs-2015-0044

Martindale, M. Q., & Henry, J. Q. (2015). Ctenophora. In A. Wanninger (Ed.), *Evolutionary Developmental Biology of Invertebrates 1: Introduction, Non-Bilateria, Acoelomorpha, Xenoturbellida, Chaetognatha* (pp. 179–201). Springer. https://doi.org/10.1007/978-3-7091-1862-7_8

Melle, W., & Skjoldal, H. R. (1998). Reproduction and development of Calanus finmarchicus, C. glacialis and C. hyperboreus in the Barents Sea. *Marine Ecology Progress Series*, *169*, 211–228. https://doi.org/10.3354/meps169211

Mills, C. E., & Haddock, S. H. D. (2007). Ctenophora. In *Ctenophora* (pp. 189–199). University of California Press. https://doi.org/10.1525/9780520930438-015

Mutlu, E. (1996). Effect of Formaldehyde on the Gelatinous Zooplankton (Pleurobrachia pileus, Aurelia aurita) During Preservation. *Turkish Journal of Zoology*, *20*(4), 423–426. https://doi.org/-

Nelson, M. M., Phleger, C. F., Mooney, B. D., & Nichols, P. D. (2000). Lipids of gelatinous antarctic zooplankton: Cnidaria and Ctenophora. *Lipids*, *35*(5), 551–559. https://doi.org/10.1007/s11745-000-555-5

Neuhäuser, M. (2011). Wilcoxon–Mann–Whitney Test. In M. Lovric (Ed.), *International Encyclopedia of Statistical Science* (pp. 1656–1658). Springer. https://doi.org/10.1007/978-3-642-04898-2_615

Nilssen, F. (2003). Economic Co-operation in the Barents Region: Russian-Norwegian Trade in the Fishing Industry. In L. Hedegaard, B. Lindström, P. Joenniemi, H. Eskelinen, K. Peschel, & C.-E. Stålvant (Eds.), *The NEBI Yearbook 2003: North European and Baltic Sea Integration* (pp. 151–164). Springer. https://doi.org/10.1007/978-3-642-59341-3_11

Oguz, T., & Gilbert, D. (2007). Abrupt transitions of the top-down controlled Black Sea pelagic ecosystem during 1960–2000: Evidence for regime-shifts under strong fishery exploitation and nutrient enrichment modulated by climate-induced variations. *Deep Sea Research Part I: Oceanographic Research Papers*, *54*(2), 220–242.

Oksanen, J., Blanchet, F. G., Friendly, M., Kindt, R., Legendre, P., McGlinn, D., Minchin, P. R., O'hara, R. B., Simpson, G. L., & Solymos, P. (2019). Vegan: Community ecology package (version 2.5-6). *The Comprehensive R Archive Network*.

Ortman, B. D. (2008). *DNA barcoding the Medusozoa and Ctenophora*. University of Connecticut.

Ortman, B. D., Bucklin, A., Pagès, F., & Youngbluth, M. (2010). DNA Barcoding the Medusozoa using mtCOI. *Deep Sea Research Part II: Topical Studies in Oceanography*, *57*(24), 2148–2156. https://doi.org/10.1016/j.dsr2.2010.09.017

Pagès, F., González, H., & González. (1996). Diet of the gelatinous zooplankton in Hardangerfjord (Norway) and potential predatory impact by Aglantha digitale (Trachymedusae). *Marine Ecology Progress Series*, *139*, 69–77. https://doi.org/10.3354/meps139069

Paley, A., & Beemer, J. (2021). *A Study of the Feeding and Predatory Behavior of the Ctenophore Beroe abyssicola*. https://digital.lib.washington.edu:443/researchworks/handle/1773/47146

Pantiukhin, D., Verhaegen, G., Kraan, C., Jerosch, K., Neitzel, P., Hoving, H.-J. T., & Havermans, C. (2023). Optical observations and spatio-temporal projections of gelatinous zooplankton in the Fram Strait, a gateway to a changing Arctic Ocean. *Frontiers in Marine Science*, *10*, 804.

Pedersen, S. A., & Smidt, E. L. B. (2000). Zooplankton distribution and abundance in West Greenland waters, 1950-1984. *Journal of Northwest Atlantic Fishery Science*, *26*.

Pertsova, N. M., Kosobokova, K. N., & Prudkovsky, A. A. (2006). Population size structure, spatial distribution, and life cycle of the hydromedusa Aglantha digitale (O.F. Müller, 1766) in the White Sea. *Oceanology*, *46*(2), 228–237. https://doi.org/10.1134/S0001437006020093

Pierson, J., Camatti, E., Hood, R., Kogovšek, T., Lučić, D., Tirelli, V., & Malej, A. (2020). Mesozooplankton and Gelatinous Zooplankton in the Face of Environmental Stressors. In *Coastal Ecosystems in Transition* (pp. 105–127). American Geophysical Union (AGU). https://doi.org/10.1002/9781119543626.ch6

Pitt, K. A., & Lucas, C. H. (2014). *Jellyfish blooms*. Springer.

Podar, M., Haddock, S. H. D., Sogin, M. L., & Harbison, G. R. (2001). A Molecular Phylogenetic Framework for the Phylum Ctenophora Using 18S rRNA Genes. *Molecular Phylogenetics and Evolution*, *21*(2), 218–230. https://doi.org/10.1006/mpev.2001.1036

Purcell, J. E., & Arai, M. N. (2001). Interactions of pelagic cnidarians and ctenophores with fish: A review. *Hydrobiologia*, *451*(1), 27–44.

Purcell, J. E., Hoover, R. A., & Schwarck, N. T. (2009). Interannual variation of strobilation by the scyphozoan Aurelia labiata in relation to polyp density, temperature, salinity, and light conditions in situ. *Marine Ecology Progress Series*, *375*, 139–149. https://doi.org/10.3354/meps07785

Rao, C. R. (1995). A review of canonical coordinates and an alternative to correspondence analysis using Hellinger distance. *Qüestiió: Quaderns d'estadística i Investigació Operativa*.

Raskoff, K. A., Hopcroft, R. R., Kosobokova, K. N., Purcell, J. E., & Youngbluth, M. (2010). Jellies under ice: ROV observations from the Arctic 2005 hidden ocean expedition. *Deep Sea Research Part II: Topical Studies in Oceanography*, *57*(1), 111–126. https://doi.org/10.1016/j.dsr2.2009.08.010

Raskoff, K. A., Purcell, J. E., & Hopcroft, R. R. (2005). Gelatinous zooplankton of the Arctic Ocean: In situ observations under the ice. *Polar Biology*, *28*(3), 207–217. https://doi.org/10.1007/s00300-004-0677-2

Raskoff, K., Sommer, F., Hamner, W., & Cross, K. (2003). Collection and Culture Techniques for Gelatinous Zooplankton. *The Biological Bulletin*, *204*, 68–80. https://doi.org/10.2307/1543497

Reeve, M. R., & Walter, M. A. (1979). Nutritional ecology of ctenophores—A review of recent research. *Advances in Marine Biology*, *15*, 249–287.

Reeve, M. R., Walter, M. A., & Ikeda, T. (1978). Laboratory studies of ingestion and food utilization in lobate and tentaculate ctenophores 1. *Limnology and Oceanography*, *23*(4), 740–751. https://doi.org/10.4319/lo.1978.23.4.0740

Rey, F. (1985). The influence of ice and hydrographic conditions on the development of phytoplankton in the Barenz Sea. *Marine Biology of Polar Regions and Effects of Stress on Marine Organisms*, 49–63.

Ronowicz, M., Kukliński, P., & Mapstone, G. M. (2015). Trends in the Diversity, Distribution and Life History Strategy of Arctic Hydrozoa (Cnidaria). *PLOS ONE*, *10*(3), e0120204. https://doi.org/10.1371/journal.pone.0120204

Rossi, S., Gravili, C., Milisenda, G., Bosch-Belmar, M., De Vito, D., & Piraino, S. (2019). Effects of global warming on reproduction and potential dispersal of Mediterranean Cnidarians. *The European Zoological Journal*, *86*(1), 255–271. https://doi.org/10.1080/24750263.2019.1631893

Rudels, B., Korhonen, M., Schauer, U., Pisarev, S., Rabe, B., & Wisotzki, A. (2015). Circulation and transformation of Atlantic water in the Eurasian Basin and the contribution of the Fram Strait inflow branch to the Arctic Ocean heat budget. *Progress in Oceanography*, *132*, 128–152. https://doi.org/10.1016/j.pocean.2014.04.003

Sakshaug, E., Johnsen, G. H., & Kovacs, K. M. (2009). *Ecosystem Barents Sea*. Tapir Academic Press.

Sampei, M., Forest, A., Sasaki, H., Hattori, H., Makabe, R., Fukuchi, M., & Fortier, L. (2009). Attenuation of the vertical flux of copepod fecal pellets under Arctic sea ice: Evidence for an active detrital food web in winter. *Polar Biology*, *32*(2), 225–232. https://doi.org/10.1007/s00300-008-0523-z

Sanger, F., Nicklen, S., & Coulson, A. R. (1977). DNA sequencing with chain-terminating inhibitors. *Proceedings of the National Academy of Sciences*, *74*(12), 5463–5467. https://doi.org/10.1073/pnas.74.12.5463

Seuthe, L., Darnis, G., Riser, C. W., Wassmann, P., & Fortier, L. (2007). Winter–spring feeding and metabolism of Arctic copepods: Insights from faecal pellet production and respiration measurements in the southeastern Beaufort Sea. *Polar Biology*, *30*(4), 427–436. https://doi.org/10.1007/s00300-006-0199-1

Shiganova, T. A., & Abyzova, G. A. (2022). Revision of Beroidae (Ctenophora) in the southern seas of Europe: Systematics and distribution based on genetics and morphology. *Zoological*

Journal of the Linnean Society, *194*(1), 297–322. https://doi.org/10.1093/zoolinnean/zlab021

Siferd, T. D., & Conover, R. J. (1992). Natural history of ctenophores in the Resolute Passage area of the Canadian High Arctic with special reference to Mertensia ovum. *Marine Ecology Progress Series*, *86*(2), 133–144.

Skagseth, Ø. (2008). Recirculation of Atlantic Water in the western Barents Sea. *Geophysical Research Letters*, *35*(11). https://doi.org/10.1029/2008GL033785

Slagstad, D., Wassmann, P. F. J., & Ellingsen, I. (2015). Physical constrains and productivity in the future Arctic Ocean. *Frontiers in Marine Science*, *2*. https://www.frontiersin.org/articles/10.3389/fmars.2015.00085

Steinberg, D. K., & Saba, G. K. (2008). Chapter 26—Nitrogen Consumption and Metabolism in Marine Zooplankton. In D. G. Capone, D. A. Bronk, M. R. Mulholland, & E. J. Carpenter (Eds.), *Nitrogen in the Marine Environment (Second Edition)* (pp. 1135–1196). Academic Press. https://doi.org/10.1016/B978-0-12-372522-6.00026-8

Sundfjord, A., Assmann, K. M., Lundesgaard, Ø., Renner, A. H., Lind, S., & Ingvaldsen, R. B. (2020). Suggested water mass definitions for the central and northern Barents Sea, and the adjacent Nansen Basin: Workshop Report. *The Nansen Legacy Report Series*, *8*.

Swanberg, N. (1974). The feeding behavior of Beroe ovata. *Marine Biology*, *24*(1), 69–76. https://doi.org/10.1007/BF00402849

Swanberg, N., & Båmstedt, U. (1991a). Ctenophora in the Arctic: The abundance, distribution and predatory impact of the cydippid ctenophore Mertensia ovum (Fabricius) in the Barents Sea. *Polar Research*, *10*(2), 507–524.

Swanberg, N., & Båmstedt, U. (1991b). The role of prey stratification in the predation pressure by the cydippid ctenophore Mertensia ovum in the Barents Sea. In R. B. Williams, P. F. S. Cornelius, R. G. Hughes, & E. A. Robson (Eds.), *Coelenterate Biology: Recent Research on Cnidaria and Ctenophora* (pp. 343–349). Springer Netherlands. https://doi.org/10.1007/978-94-011-3240-4_49

Tamm, S. L., & Tamm, S. (1993). Diversity of macrociliary size, tooth patterns, and distribution in Beroe (Ctenophora). *Zoomorphology*, *113*(2), 79–89. https://doi.org/10.1007/bf00403086

Thein, H., Ikeda, H., & Uye, S. (2013). Ecophysiological characteristics of podocysts in Chrysaora pacifica (Goette) and Cyanea nozakii Kishinouye (Cnidaria: Scyphozoa: Semaeostomeae): Effects of environmental factors on their production, dormancy and excystment. *Journal of Experimental Marine Biology and Ecology*, *446*, 151–158. https://doi.org/10.1016/j.jembe.2013.05.013

Tremblay, J.-É., Bélanger, S., Barber, D. G., Asplin, M., Martin, J., Darnis, G., Fortier, L., Gratton, Y., Link, H., Archambault, P., Sallon, A., Michel, C., Williams, W. J., Philippe, B., & Gosselin, M. (2011). Climate forcing multiplies biological productivity in the coastal Arctic Ocean. *Geophysical Research Letters*, *38*(18). https://doi.org/10.1029/2011GL048825

Troedsson, C., Bouquet, J.-M., Aksnes, D. L., & Thompson, E. M. (2002). Resource allocation between somatic growth and reproductive output in the pelagic chordate Oikopleura dioica allows opportunistic response to nutritional variation. *Marine Ecology Progress Series*, *243*, 83–91.

Urban, P., Præbel, K., Bhat, S., Dierking, J., & Wangensteen, O. S. (2022). DNA metabarcoding reveals the importance of gelatinous zooplankton in the diet of Pandalus borealis, a keystone species in the Arctic. *Molecular Ecology*, *31*(5), 1562–1576. https://doi.org/10.1111/mec.16332

Verity, P., & Smetacek, V. (1996). Organism life cycles, predation, and the structure of marine pelagic ecosystems. *Marine Ecology Progress Series*, *130*, 277–293. https://doi.org/10.3354/meps130277

Wassmann, P., Ratkova, T., Andreassen, I., Vernet, M., Pedersen, G., & Rey, F. (1999). Spring Bloom Development in the Marginal Ice Zone and the Central Barents Sea. *Marine Ecology*, *20*(3–4), 321–346. https://doi.org/10.1046/j.1439-0485.1999.2034081.x

Yaragina, N. A., Stige, L. C., & Langangen, Ø. (2021). Bycatch data from ichthyoplankton surveys reveal long-term trends in gelatinous zooplankton in the Norwegian and Barents Seas. *ICES Journal of Marine Science*, *79*(3), 868–881. https://doi.org/10.1093/icesjms/fsab225

Yilmaz, I. N. (2015). Collapse of zooplankton stocks during Liriope tetraphylla (Hydromedusa) blooms and dense mucilaginous aggregations in a thermohaline stratified basin. *Marine Ecology*, *36*(3), 595–610.

Zelickman, E. A. (1972). Distribution and ecology of the pelagic hydromedusae, siphonophores and ctenophores of the Barents Sea, based on perennial plankton collections. *Marine Biology*, *17*(3), 256–264. https://doi.org/10.1007/BF00366301

Zwickl, D. J. (2006). *Genetic algorithm approaches for the phylogenetic analysis of large biological sequence datasets under the maximum likelihood criterion* [Thesis]. https://repositories.lib.utexas.edu/handle/2152/2666

Appendix

Appendix 1

Appendix 1 – Pre PCR lab in Trondheim Biological Station.

Appendix 2

Appendix 2 – Post PCR lab in Trondheim Biological Station.

Appendix 3

DNA extraction protocol:

- Add 50 µL of 6% Chelex solution (mixed beforehand) to the Eppendorf tissue sample tube.
- Mix the solution with vibrofix VF1 electronics for around 7 seconds.
- Heat the solution for 10 minutes at 98 degrees Celsius with the lits pierced.
- Centrifuge at 15 000 $n.min^{-1}$ for 10 minutes.
- Take the surfactant, being careful not to take any Chelex particle, and transfer it to a new DNA free Eppendorf tube.

Mastermix recipe:

- 1 µL of forward primer (diluted 10 times)
- 1µL of reverse primer (diluted 10 times)
- 4 µL of 5x buffer
- 0.4 µL of dNTP 10 mM
- 0.6 µL of 3% DMSO
- 11.6 µL of H2O Q (Nuclease free water)
- 0.4 µL of Phire enzyme

Mastermix protocol:

- Thaw the components of the master mix outside the freezer (except Phire enzyme).
- Mix them briefly.
- Add the components of the master mix following the order of the recipe in a DNA free Eppendorf.
- Keep it in the ice.
- Take out the Phire enzyme from the freezer.
- Add it to the master mix, homogenize with the pipette.
- Put the master mix back in the ice and the Phire enzyme in the freezer.

Kober primers PCR cycles (Kober & Nichols, 2007):

- First denaturation: 98°C for 5 minutes.
- Denaturation: 98°C for 8 seconds.
- Anhiling: 56°C for 10 seconds.
- Synthesis: 72°C for 1 minute.

} × 40

- Final synthesis: 72°C for 5 minutes.
- Conservation: 4°C until the strip is taken out of the machine.

Electrophoresis gel protocol:

- Make a big gel (60 wells).

- Mix 1.8g of Agarose and 120mL of Buffer 1/50 TAE.
- Cook and mix until complete dissolution of the Agarose.
- Add 12 µL of Sybr safe.
- Pour into a big gel mold (60 wells).
- Wait until gel set (~30minutes).

- Make a small gel (30 wells).
  - Mix 0.8g of Agarose and 50mL of Buffer 1/50 TAE.
  - Cook and mix until complete dissolution of the Agarose.
  - Add 5µL of Sybr safe.
  - Pour into a small mold (30 wells).
  - Wait until the gel set (~30minutes).

DNA purification (Cytiva GFX^{tm} PCR DNA and gel purification kit):

1) Sample capture
   - Add 500µL of **Capture buffer type 3** in new labeled DNA free Eppendorf tubes (Use one pipette tip).
   - Add 15 µL of your amplified DNA sample in its respective labeled Eppendorf tube and mix with the pipette (Change pipette tip between samples).
   - Check that the color of the mix is yellow or pale orange.
   - Assemble and label for each purification to be performed a GFX Microspin column and a collection tube.
2) Sample binding
   - Centrifuge the **Capture buffer type 3**-sample mix, to make sure the liquid is at the bottom of the tube.
   - Load the **Capture buffer type 3**-sample mix in its respective labeled assembled GFX Microspin column and collection tube (Change pipette tip between samples).
   - Cap the GFX Microspin column with the lids of the collection tube.
   - Spin the assemblage at 16 000 x g for 30sec. This couldn't be done with the TBS centrifuge; hence it was spined at 15 000 x g for 1 minute (~30 sec was required to reach 15 000 x g).
   - Discard the flow through by emptying the collection tube and place the GFX Microspin column back inside the collection tube.
3) Wash and dry
   - Add 500µL of **Wash buffer type 1** (Make sure this buffer was diluted with 250mL of ethanol before) to the GFX Microspin column (Use one pipette tip, but if the pipette tip touches the column, change the pipette tip).
   - Cap the GFX Microspin column with the lids of the collection tube.
   - Spin the assemblage at 16 000 x g for 30sec. Again, it wasn't possible so, the assemblage was spined at 15 000 x g for 1 minute.
   - Discard the collection tube and transfer the GFX Microspin column to a fresh DNase-free 1.5mL microcentrifuge tube.
4) Elution
   - Add 25µL of **Elution buffer type 6** to the center of the membrane in the assembled GFX Microspin column and sample tube (Use one pipette tip, but if the pipette tip touches the column, change the pipette tip).
   - Incubate the assemblage for 1minute at room temperature.

- Spin the assemblage at 16 000 x g for 1minute to recover the purified DNA. To compensate for the 30secondes needed to reach 15 000 x g the assemblage was spin at 15 000 x g for 1minute and 30seconds.
- Discard the GFX Microspin column and store the purified DNA sample at -20°C.

Appendix 4

Appendix 4 – Electrophoresis gel picture. It display the 50 bp DNA Ladder (ladder), a well and a detection band. Presence of a detection band display the PCR success.

Appendix 5

Appendix 5 – MIK net abundance matrix. Gelatinous zooplankton MIK net abundance for all stations (P1 to P7) and seasons (August 2019, December 2019, March 2021 and May 2021). Rare taxa were excluded and Sarsia species were grouped under Sarsia sp.

Cruise	Station	ID	Aglantha digitale	Beroe sp.	Euphysa flammea	Cyclophilia	Sarsia sp.	Mertensia ovum	Ptychogena lactea	Atolla tenella	Botrynema brucei	Botrynema ellinorae	Unknown	Bougainvillia superciliaris
Q1	P1	Q1_P1												
Q1	P2	Q1_P2	0.0803											
Q1	P3	Q1_P3	0.0034			0.00934		0.00016	0.00113					
Q1	P4	Q1_P4						0.02603						
Q1	P5	Q1_P5												
Q1	P6	Q1_P6	0.01008	0.00187				0.00112					0.00075	
Q1	P7	Q1_P7	0.01683	0.00005				0.00032				0.0019		
Q3	P1	Q3_P1												
Q3	P2	Q3_P2		0.03571			0.01587	0.01587						
Q3	P3	Q3_P3	0.05911	0.00766				0.00657	0.00219					
Q3	P4	Q3_P4		0.00673		0.0077		0.00289	0.00096					
Q3	P5	Q3_P5		0.00481		0.01732								
Q3	P6	Q3_P6												
Q3	P7	Q3_P7	0.01385	0.00032		0.00032		0.00032		0.00032	0.00032	0.00032	0.00032	
Q4	P1	Q4_P1	0.08677	0.01058				0.01474						
Q1	P2	Q4_P2			0.00934			0.02611	0.00373					
Q4	P3	Q4_P3	0.0102	0.02494										
Q4	P4	Q4_P4		0.00106	0.02212								0.00317	
Q4	P5	Q4_P5	0.00285				0.00397		0.00285					0.00285
Q4	P6	Q4_P6	0.02033	4e-04				0.00198					0.00159	
Q4	P7	Q4_P7	0.00317									0.00063		

Appendix 6

Appendix 6 – MultiNet abundance matrix. Gelatinous zooplankton MultiNet abundance for all stations (P1 to P7) and seasons (August 2019, December 2019, March 2021 and May 2021). Rare taxa were excluded, Hydrozoa refer to Hydrozoa larvae.

Cruise	Station	ID	Hydrozoa	Oikopleura	Fritillaria borealis	Aeglnopsis laurentii	Beroe cucumis	Dimophyes arctica	Homoeonema platygonon	Aglantha digitale	Mertensia ovum	Plotocnide borealis	Euphysa flammea	Homeonema	Sarsia princeps	Hallitholus cirratus	Rathkea octopunctata
Q1	P1	Q1_P1	0.16654	0.80113	0.23427	0.09056	0.07509			0.01155							
Q1	P2	Q1_P2		6.95015	3.51905	0.0676	0.0199			0.0507							
Q1	P3	Q1_P3		0.89575	0.07618	2.56859		3.74936		0.03221	0.03809						
Q1	P4	Q1_P4		1.16778	0.69333	2.28256	0.07864	0.03688	0.27844	0.05894	0.2239						
Q1	P5	Q1_P5		0.54669		0.90295	1.12432			0.02333	0.2032						
Q1	P6	Q1_P6		0.18815	0.74144	0.00351	0.0128	0.04525	0.03158	0.00699							
Q1	P7	Q1_P7	0.0095	0.26953	0.20841	0.07101	0.00093	0.00279	0.06917	0.00056							
Q2	P1	Q2_P1	4.42467	0.05925	2.52476		0.1463					0.83298					
Q2	P2	Q2_P2		0.6296	1.91377	1.30434	0.5238	0.05216					0.06219				
Q2	P3	Q2_P3		0.03013		3.29476	0.16868	0.03026	0.15084			0.3618					
Q2	P4	Q2_P4	0.19533	0.41043	0.424	3.22793	0.14877	0.55492	0.41859	0.01893							
Q2	P5	Q2_P5		0.54231	0.11392	1.78155	0.0217	0.05493		0.01899		0.05696					
Q2	P6	Q2_P6	0.50235	0.6096	1.98354		0.03421	0.05321		0.0095	0.04276						
Q2	P7	Q2_P7	0.04389	0.17389	0.10626	0.05679		0.01378	0.01374								
Q3	P1	Q3_P1		10.49179	151.63331		0.04926			0.08821	0.23797						3.13787
Q3	P2	Q3_P2		8.13279	0.18164	0.32018									0.0561	0.03532	
Q3	P3	Q3_P3		3.54719	0.20458	0.54955				0.09402							
Q3	P4	Q3_P4	0.39401	6.95811	0.08824	0.35013		0.0182		0.04597					0.06084		
Q3	P5	Q3_P5		2.12414	14.2529	0.36367						0.37739					
Q3	P6	Q3_P6	0.50133	6.56309	26.98577			0.06491		0.29435							
Q3	P7	Q3_P7		0.04737	0.14054	0.00696	0.01592	0.02876		0.01313				0.34894			
Q4	P1	Q4_P1		0.016			0.47737			0.09673							
Q4	P2	Q4_P2		21.32476		0.12177				0.03597	0.11265	1.31975					
Q4	P3	Q4_P3		7.80289		1.8934	1.0589			0.03198		0.37367					
Q4	P4	Q4_P4		5.64485	0.45569	0.5235		0.00911				0.45569					
Q4	P5	Q4_P5		5.99495		1.80373				0.02241		1.24802					
Q4	P6	Q4_P6		0.92052	1.08317			0.11182	0.28253	0.00677							
Q4	P7	Q4_P7		0.01564	0.22192	0.02316		0.00702	0.09389	0.0098							

Appendix 7

Appendix 7 – Environmental variable for all stations (P1 to P7) and seasons (August 2019, December 2019, March 2021 and May 2021).

Cruise	Station	ID	Latitude	Longitude	Bottom depth (m)	Mean temperature (°C)	Mean salinity (g L^{-1})	Percentage AW (%)	Percentage PW (%)	Percentage wPW (%)	Total zooplankton biomass (mg m^{-3})	Chlorophyll a stock (mg m^{-2})	Day of the year	Microzooplankton biomass (µC m^{-3})
Q1	P1	Q1_P1	76.00	31.22	325	1.43	69.84	0.00	0.00	30.16	1.42	0.46	63	0.04
Q1	P2	Q1_P2	77.50	33.93	192	-0.92	0.00	64.64	0.00	35.36	7.44	0.42	66	0.12
Q1	P3	Q1_P3	78.75	34.00	305	-0.46	0.00	41.95	0.00	58.05	20.86	0.43	67	0.05
Q1	P4	Q1_P4	79.78	33.67	324	0.42	0.00	33.55	0.00	66.45	49.95	0.43	70	0.04
Q1	P5	Q1_P5	80.48	34.14	156	-1.25	0.00	96.21	0.00	3.79	35.41	0.44	71	0.02
Q1	P6	Q1_P6	81.54	30.86	850	1.64	50.00	1.92	0.00	48.08	11.71	0.65	75	0.03
Q1	P7	Q1_P7	81.99	29.91	3297	-0.20	16.82	1.31	75.66	6.21	4.79	0.86	76	0.02
Q2	P1	Q2_P1	76.00	31.22	326	1.68	100.00	0.00	0.00	0.00	4.12	3.03	120	1.78
Q2	P2	Q2_P2	77.50	33.97	195	-1.48	0.00	100.00	0.00	0.00	5.05	2.27	122	1.51
Q2	P3	Q2_P3	78.74	33.95	301	-0.60	0.00	55.30	0.00	44.70	14.66	0.83	123	0.91
Q2	P4	Q2_P4	79.68	33.56	360	0.55	0.00	27.38	0.00	72.62	28.11	3.64	125	1.20
Q2	P5	Q2_P5	80.50	33.95	161	-1.01	0.00	99.35	0.00	0.65	28.90	1.05	127	1.23
Q2	P6	Q2_P6	81.55	30.85	889	0.66	65.46	9.17	0.00	25.37	8.38	3.85	132	1.76
Q2	P7	Q2_P7	81.97	30.03	3283	-0.23	16.96	2.21	75.84	5.00	1.64	0.52	134	1.17
Q3	P1	Q3_P1	76.00	31.22	324	1.83	74.29	0.00	0.00	25.71	33.30	0.99	220	2.49
Q3	P2	Q3_P2	77.50	34.00	189	-0.44	0.00	57.23	27.71	15.06	59.95	1.46	223	1.53
Q3	P3	Q3_P3	78.75	34.00	307	-1.13	0.00	64.44	5.28	6.34	34.96	0.65	225	0.80
Q3	P4	Q3_P4	79.69	34.23	353	-1.43	0.00	77.13	0.00	3.35	38.03	1.05	228	0.35
Q3	P5	Q3_P5	80.53	33.96	169	-1.33	0.00	100.00	0.00	0.00	58.25	3.11	228	1.01
Q3	P6	Q3_P6	81.55	31.16	835	1.40	77.04	6.97	7.93	8.05	14.00	11.37	230	1.96
Q3	P7	Q3_P7	81.98	29.54	3293	-0.10	22.11	1.80	74.05	2.04	3.30	1.97	232	1.50
Q4	P1	Q4_P1	76.00	31.28	322	2.38	99.67	0.00	0.00	0.33	14.46	0.07	347	0.19
Q4	P2	Q4_P2	77.50	34.01	190	-1.40	0.00	100.00	0.00	0.00	62.92	0.03	344	0.10
Q4	P3	Q4_P3	78.75	33.99	306	-1.48	0.00	81.49	0.00	0.00	24.69	0.02	343	0.36
Q4	P4	Q4_P4	79.78	34.05	326	-0.87	0.00	61.39	0.00	27.72	47.22	0.03	342	0.04
Q4	P5	Q4_P5	80.53	34.36	150	-0.70	0.00	66.94	0.00	33.06	40.74	0.03	340	0.10
Q4	P6	Q4_P6	81.55	30.87	869	1.75	82.81	4.65	5.23	7.32	11.43	0.08	339	0.16
Q4	P7	Q4_P7	82.07	28.50	3547	-0.23	17.11	1.99	77.98	2.91	6.74	0.08	337	0.31

Appendix 8

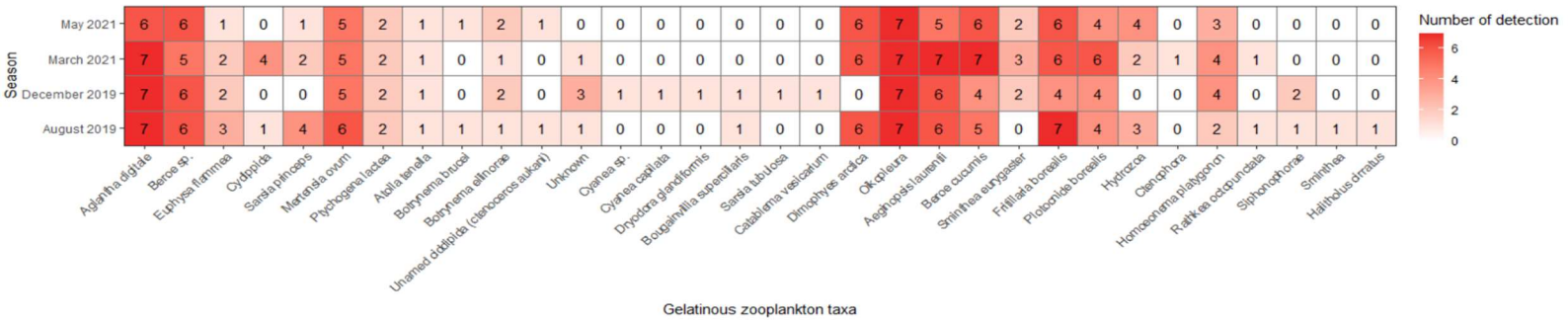

Appendix 8 - Number of detection in August 2019, December 2019, March 2021 and May 2021 of all gelatinous zooplankton taxa. The color range from white (not detected) to red (detected in every station). Taxa are common when recorded in more than two seasons and in more than four stations at least once. Based from both Multinet and MIK net data.

Appendix 9

Appendix 9A

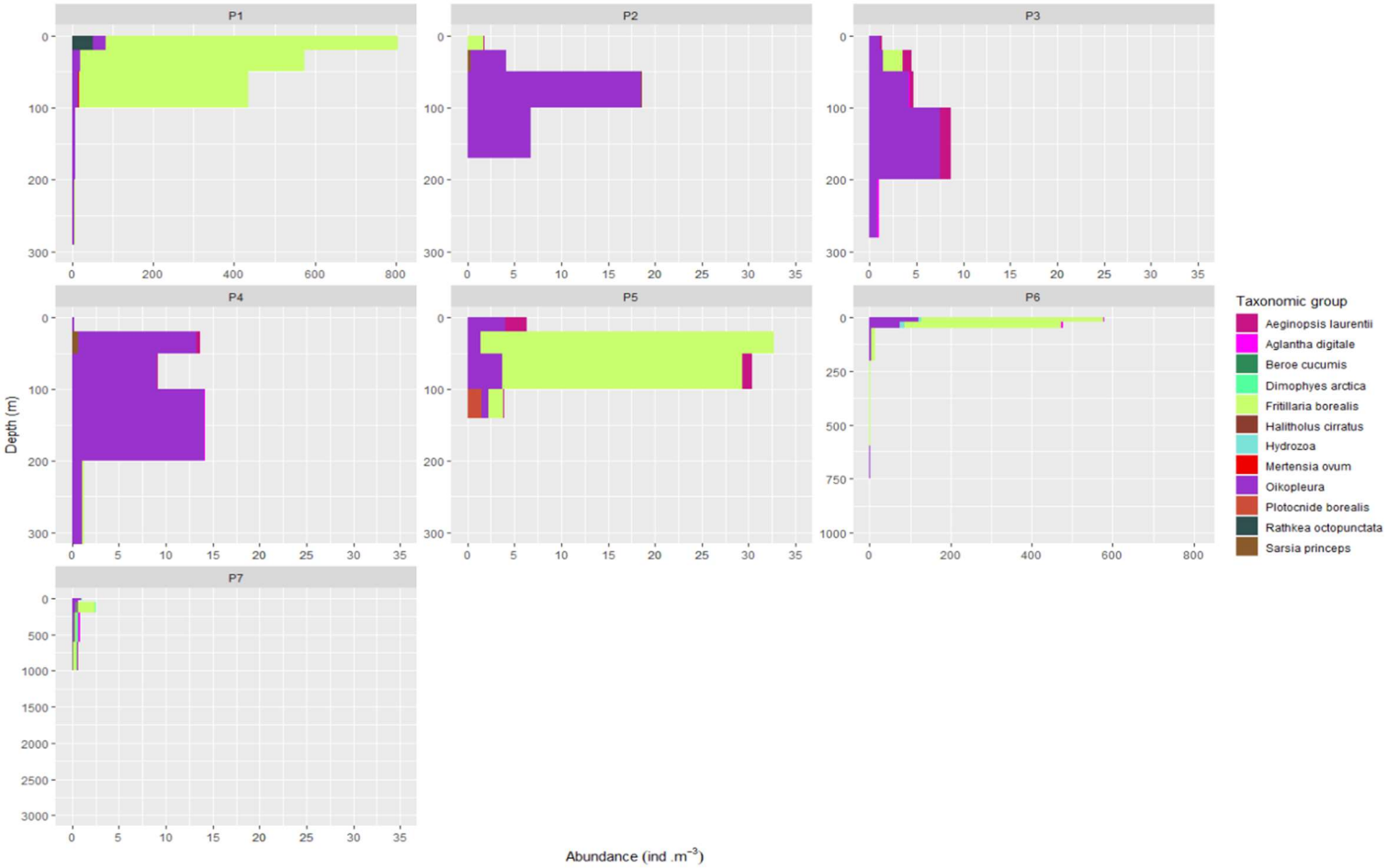

Appendix 9A – Gelatinous zooplankton vertical distribution along the transect (P1-P7) in August 2019. Data from the MultiNet 180µm and colored by taxonomic groups. For the shelf stations (P1, P2, P3, P4, P5) the maximum depth displayed is 300m and for the off-shelf stations (P6, P7) the whole water column is displayed.

Appendix 9B

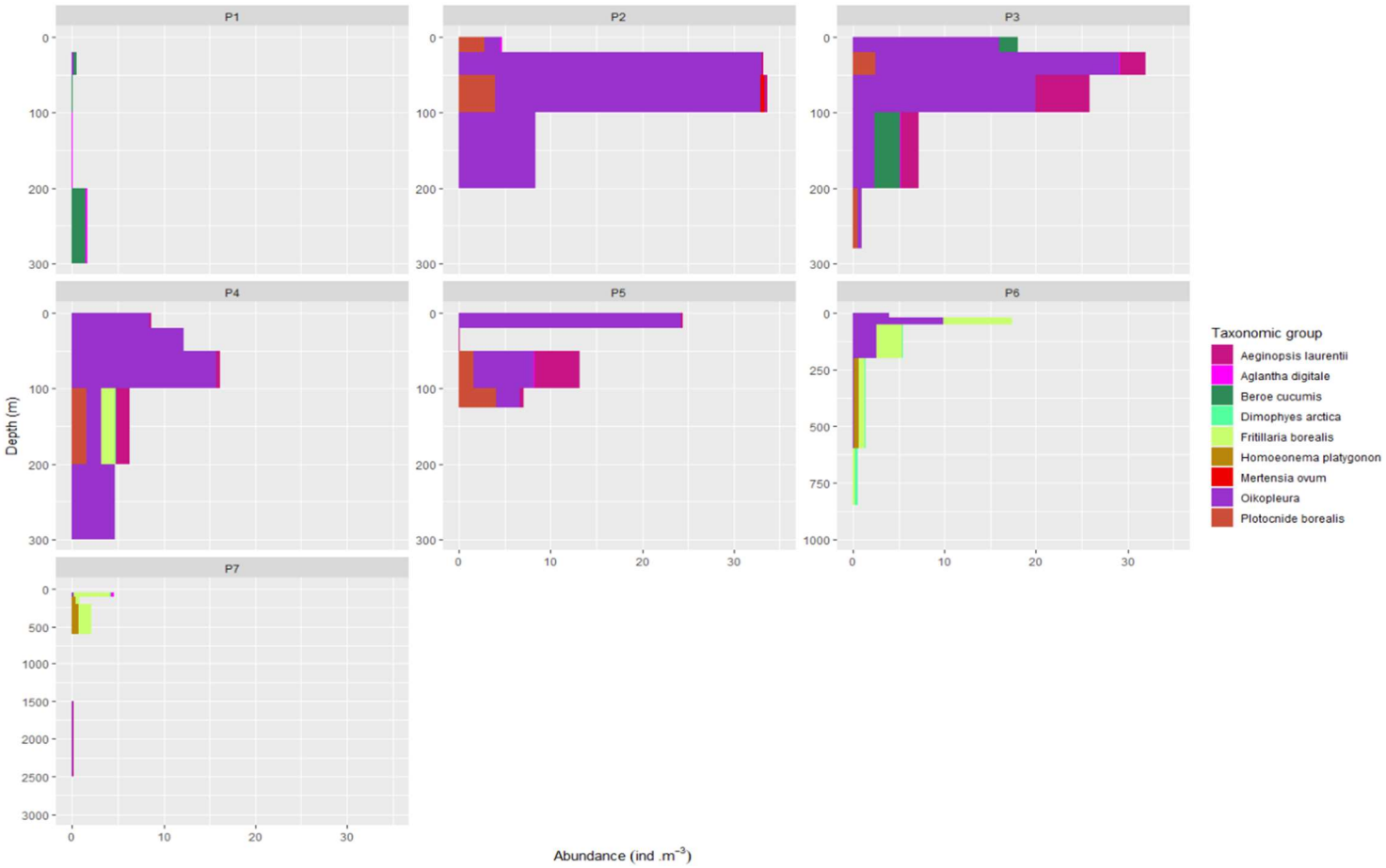

Appendix 9B - Gelatinous zooplankton vertical distribution along the transect (P1-P7) in December 2019. Data from the MultiNet 180µm and colored by taxonomic groups. For the shelf stations (P1, P2, P3, P4, P5) the maximum depth displayed is 300m and for the off-shelf stations (P6, P7) the whole water column is displayed.

Appendix 9C

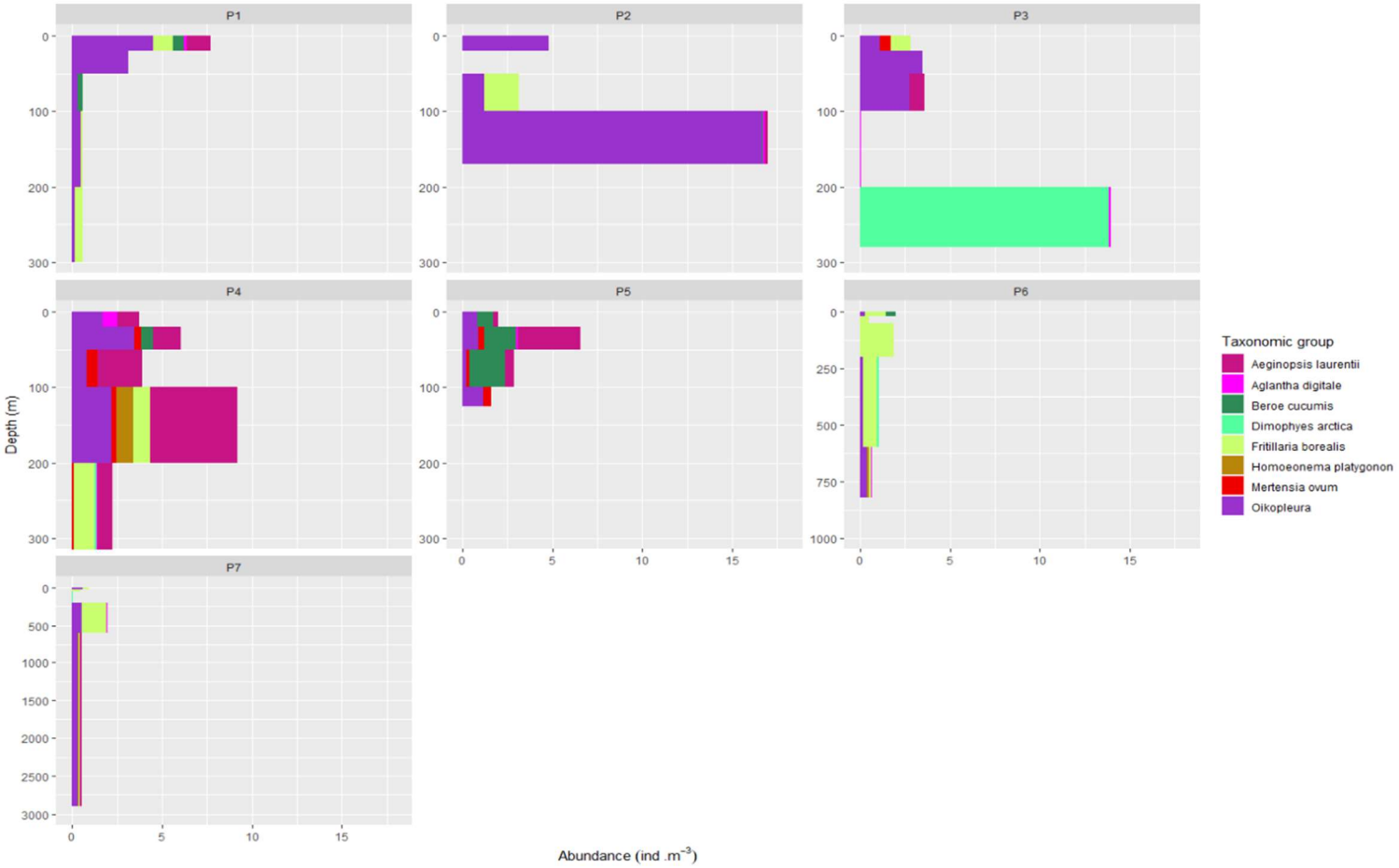

Appendix 9C - Gelatinous zooplankton vertical distribution along the transect (P1-P7) in Mars 2021. Data from the MultiNet 180µm and colored by taxonomic groups. For the shelf stations (P1, P2, P3, P4, P5) the maximum depth displayed is 300m and for the off-shelf stations (P6, P7) the whole water column is displayed.

Appendix 9D

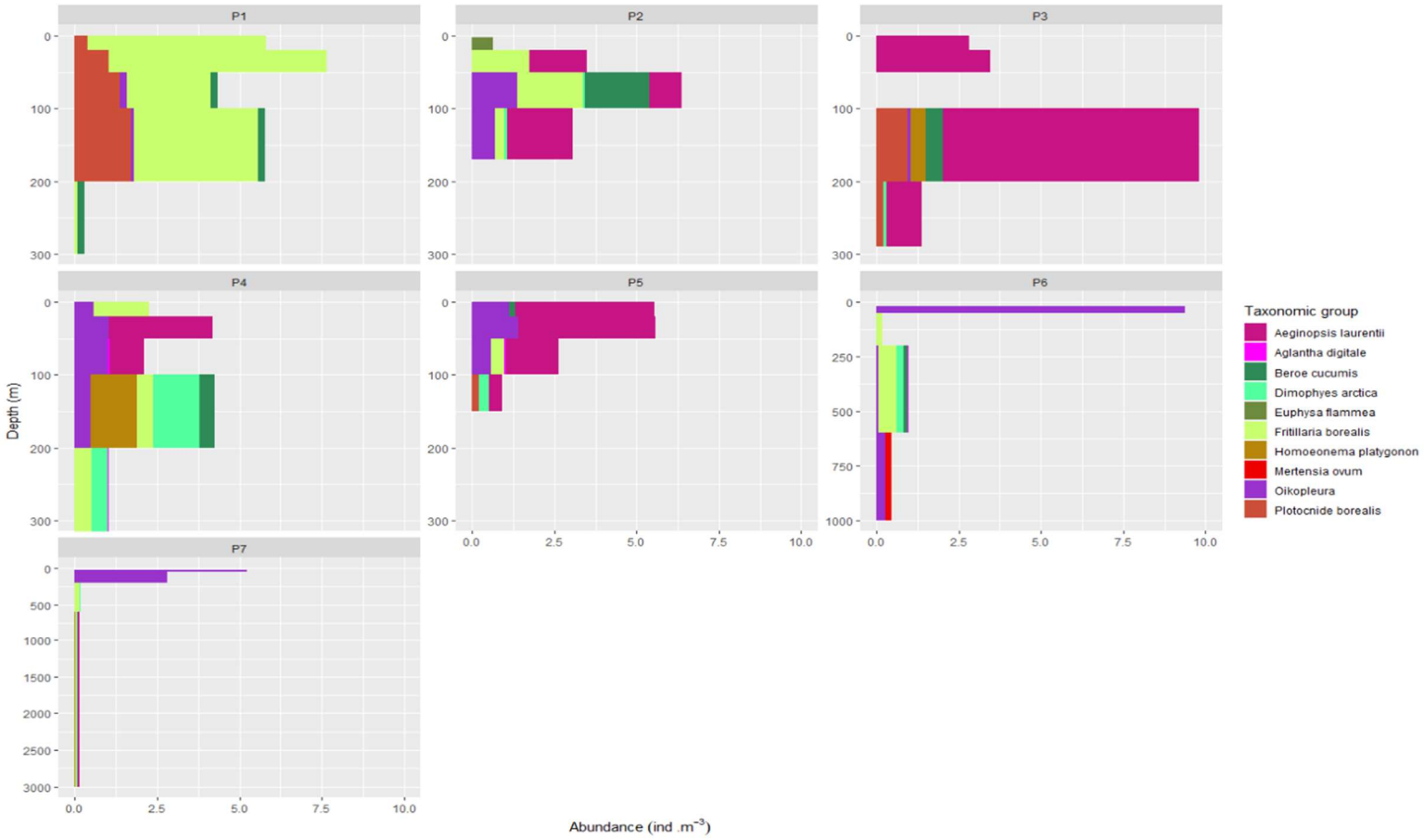

Figure 9D - Gelatinous zooplankton vertical distribution along the transect (P1-P7) in May 2021. Data from the MultiNet 180µm and colored by taxonomic groups. For the shelf stations (P1, P2, P3, P4, P5) the maximum depth displayed is 300m and for the off-shelf stations (P6, P7) the whole water column is displayed.

Appendix 10

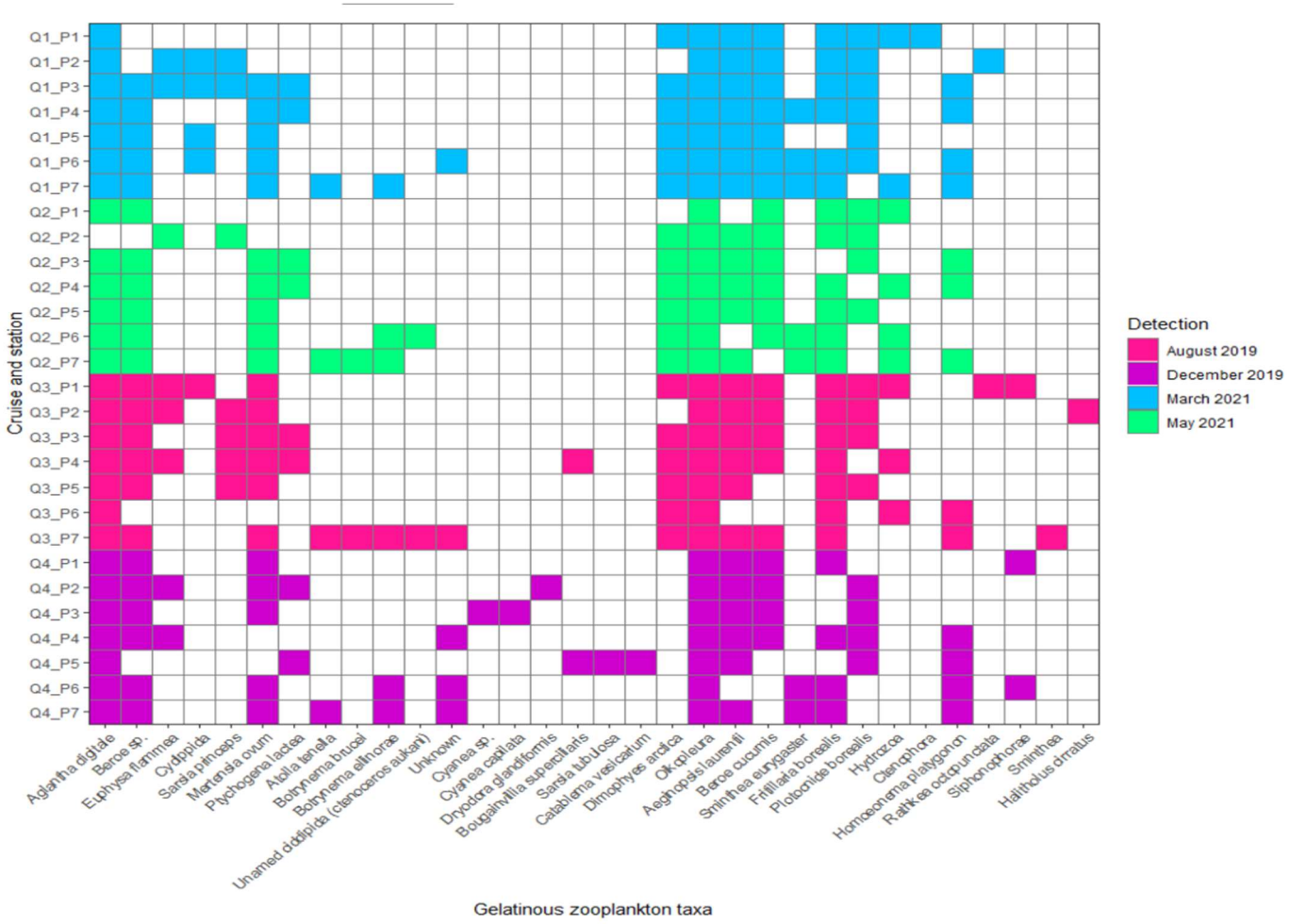

Appendix 10 – Detection/no detection of all gelatinous taxa along the transect (P1-P7) in August 2019, December 2019, March 2021 and May 2021. The colors indicate the detection. Based from both Multinet and MIK net data. Hydrozoa stand for Hydrozoa larvae.

Appendix 11

Appendix 11 – Comparaison of the morphological features before and after conservation in >96% non-denatured EtOH at -20°C.

Fresh individual	
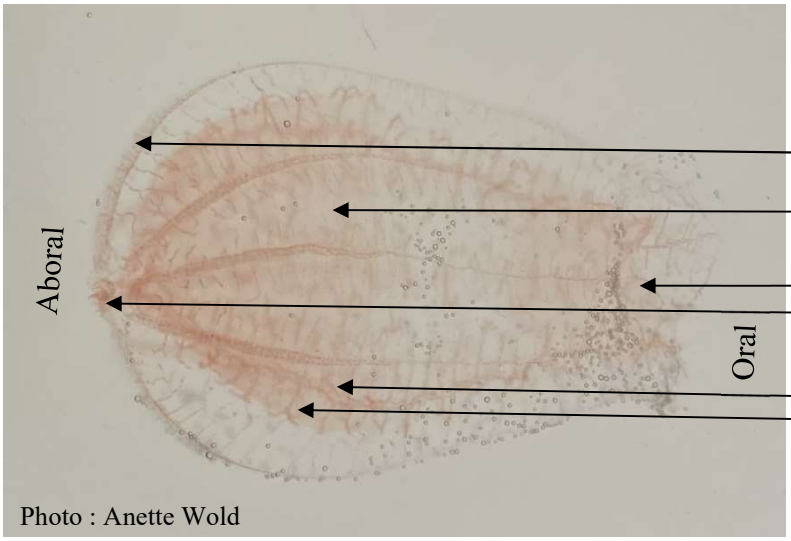	**Transparent** Ctenes Colored Stomodaeum Mouth Papillae Meridional canal Diverticule
Individuals conserved in >96% non-denatured EtOH at -20°C	
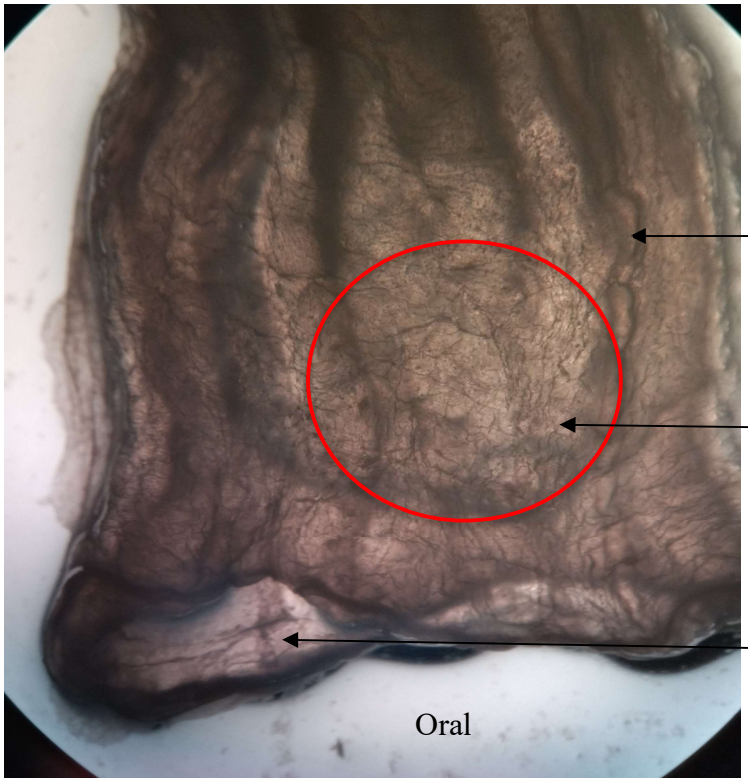	Paragastric canal? No diverticule Mouth

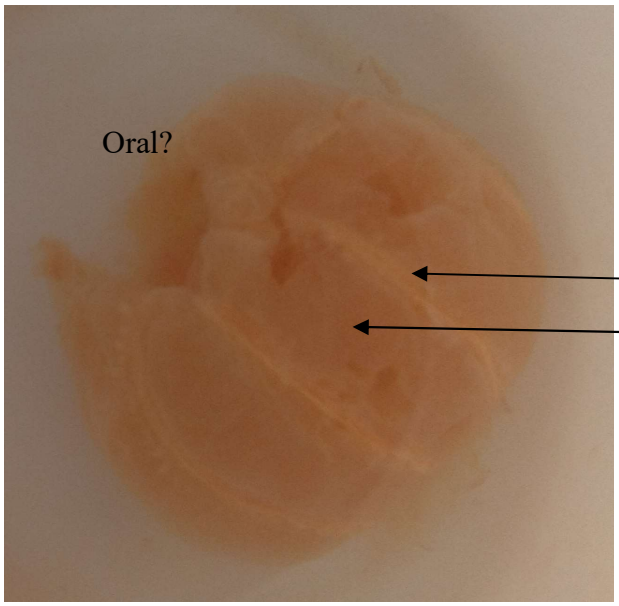

Ctenes

Opaque

Loss of the overall shape and shrink